“Electrical and Optical properties of electroluminescent materials used for Organic Light Emitting Device”

A Thesis Submitted

In partial fulfillment of the requirement
For the degree of

MASTER OF TECHNOLOGY
IN
MATERIALS SCIENCE AND ENGINEERING

BY

Arjun Singh
(Roll no. 60702001)

SCHOOL OF PHYSICS AND MATERIAL SCIENCE
THAPAR UNIVERSITY
PATIALA-147004, INDIA

CERTIFICATE

This is certify that the thesis entitled **"Electrical and optical properties of electroluminescent materials used for Organic Light Emitting Device** "submitted by **Mr. Arjun Singh** is in partial fulfillment for Degree of MASTER OF TECHNOLOGY IN MATERIAL SCIENCE AND ENGINEERING of this university. This work has been done under our supervision. The work presented in this thesis is original to the best of our knowledge and has not been submitted to any other degree of this or other any university.

This work has been carried out from **2 January 2009 to 3 July 2009**

Supervisors

Ritu Srivastava 07/07/09

Dr. Ritu Srivastava

Scientist 'C'

Centre for Organic Electronics

National Physical Laboratory

New Delhi-110012

Dr. Ritu Srivastava
Scientist 'C'
National Physical Laboratory
Dr. K. S. Krishnan Road,
New Delhi-110012 (india)

Deoijandom

Dr.D.P.Singh

School of Physics and Material Science

Thapar University

Patiala-147004

Countersigned by:

Dr.O.P.Pandey

Prof.& Head

School of Physics and Material Science

Thapar University

Patiala-147004

RK Sharma 21/7/09

Dr. R.K. Sharma

Dean ,Academic Affairs

Thapar University

Patiala-147004

ACKNOWLEDGEMENT

This master thesis work is the final examination toward getting my master degree in Material Science and Engineering at Thapar university (Patiala) Punjab. The work has been carried out within the Centre for organic Electronics at National Physical Laboratory (New Delhi) India.

I express my deep sense of gratitude to **Dr. M. N. Kamlasanan** for providing me an opportunity to work in Centre for Organic Electronics, NPL. His astonishing language skills and his clear vision of scientific content help me in tremendous manner. Words can hardly express my sense of gratitude to **Dr. Ritu Srivastava** for her invaluable supervision during the course of my thesis work. Dr. Srivastava was always available and helpful. Her great knowledge and wonderful attitude help in my training tremendously; her kindness, patience are much appreciable

I want to express my deep sense of gratitude to my supervisor **Dr. D.P. Singh**. His wide knowledge and logical way of thinking have been of great value for me.

I express my gratitude to **Prof. O. P Pandey,** Head, School of Physics and Material Science, Thapar University Patiala for his invaluable support and encouragement.

I wish to express my sincere thanks to **Dr. Vikram Kumar (Director NPL),** for permitting and providing the facilities necessary for carrying out thesis work at NPL.

Dr. A. K. Gupta, Dr. S. S. Bawa, **Dr. A. K. Aggarwal** , Head HRD group, NPL, for their support and encouragement during the course of thesis work. I am extremely thankful to Dr.Suresh Chand, Dr. S. K. Dhawan, for their invaluable help.

I also want to thanks Mr. Dharamveer Siani, from HRD group for his kind help.

I am deeply indebted to my teachers, Dr. K. K. Raina , Dr. N. K. Verma , Dr. Kulvir Singh , Dr. Sunil Kumar , Dr. Manoj Kumar, Dr. S. D. Tiwari, Dr. Loveleen Kaur , Dr.Alka Upadhaya, Dr. Puneet Sharma. Their ideals and concepts have had a remarkable influence on my understanding in the field of Material Science and Engineering.

I would like to give my special thanks to Virender Kumar Rai, Miss Gayatri Chauhan, Priyanka Tyagi, Mr. Arunandan Kumar, Miss Manisha Bajpayi , Mr.Amit kumar, Miss Rakhi, Miss Omvati members of Centre for Organic Electronics for their kind support in my work. Miss Priyanka and Mr. Arunandan helped me in all possible ways. Their timely discussions are very much appreciable. I also want to thanks my classmates Mr. Rahul Kumar , Miss Namita Gandhi and my junior & training mates Ruby Sidhu and Nancy Singla.

I want to express my heart full thanks to my most valuable friend Indu Singh .In my hard times you pushed me always in the right direction only because of your inspiration I am going towards the successful completion of my M.Tech degree.

I wish to express my warm and sincere thanks to all my friends (Specially Sushil Lakra, Mr.V.N.Shukla , Ranvir panwar, Manjeet Kumar, Arun kumar , Sandeep Kumar ,Kruna Sagar) who devoted their valuable time and helped me in all possible ways towards successful completion of this work.

I owe my most sincere gratitude to my mother, my father , my sister who honest support and obstinate love give me energy to complete this work successfully and gave me untring help during my difficult moments .They have always wanted the best for me and I admire my mother determination and sacrifice to put me through college.

Lastly I want to thanks Mr.Raju, Uncle ji and Mr.Hament kumar for their help in arranging laboratory materials during experiments.

Arjun Singh

Arjun Singh

ABSTRACT

Organic semiconductors have attracted lot of attention in technological community due to its potential applications in organic light emitting diodes (OLEDs), organic photovoltaic cells and field effect transistor etc. OLED is being considered as one of the most promising technology for flat-panel displays and in general lighting. The one of the important layer of OLED devices is the electroluminescence layer, for which polymer and small molecular weight metal chelates can be used. The small molecule based metal chelates are the appropriate candidates as they are processed by conventional vacuum deposition techniques. Small molecule based Zn metal complexes can be used in OLED devices as electron and hole transport layer. It can also be used as an emissive layer because of their wide spectral response in the visible region.

Zinc metal complex viz. {[(2-(2-hydroxyphenyl)benzoxazole)2-methyl -8-hydoxyquinoline} zinc [Zn(HPB)mq] have been synthesized and characterized by different characterization techniques (TGA, UV visible and Photoluminescence Spectroscopy). The thermo gravimetric analysis shows the degradation of Zn(HPB)mq at 350^0C. Both the photoluminescence and electroluminescence properties are extensively studied. The UV-Visible spectrum shows the absorption maxima at 380 nm. The photoluminescence spectra of the solution of Zn(HPB)mq exhibits maxima at 525 nm. Organic light emitting diode device has been fabricated with the structure ITO/α-NPD(40 nm)/Zn(HPB)mq(35 nm)/LiF(1 nm)/Al(100 nm), which shows a peak in electroluminescence at 545 nm . Moreover, electron only device of the Zinc metal complexes [Zn(HPB)mq] has been fabricated. The current –voltage characteristics of this device shows ohmic conduction at lower voltage and the space charge limited conduction is observed at higher voltage. The optical and electrical properties of Copper phthalocyanine (CuPc) have been studied.The thermo gravimetric analysis shows the degradation of CuPc at 450^0C. The UV-Vis spectrum of CuPc shows the absorption maxima shows at 270 nm and the maxima in photoluminescence of CuPc has been found at 410 nm.

The hole-only device by using CuPc as organic semiconductor has also been fabricated. The current- voltage characteristics of this organic material shows ohmic conduction at lower voltage , trap charge limited conduction (TCLC) at moderate voltage and trap free space charge limited conduction at higher voltage .The trap energy and Fermi energy from the I-V data has also been calculated. At lower voltage the traps are shallow traps and at higher voltage the traps are deep traps.

CONTENTS

LIST OF FIGURES

Chapter- 1

Chapter-3

Chapter-4

LIST OF PUBLICATIONS

Conference

1. "Synthesis and Characterization of Zn(HPB)mq as the novel electroluminescence material for Organic Light Emitting Diode" **pp. 156(2009)**

20th annual General Meeting of Material Research Society of India (MRSI) held at Saha Institute of Nuclear Physics Kolkata during February10-12,2009.

International Journal

1. "Synthesis and Characterization of Zn(HPB)mq as the novel electroluminescence material for Organic Light Emitting Diode"

Communicated in **Physica Status Solidi B.**

CHAPTER-1

INTRODUCTION

1.0 Introduction

Organic electronics is now a rapidly evolving research field with vast number of applications having high potential for commercial success. Research in this field is conducted on a largely multidisciplinary level, involving: theoretical physics and Chemistry, synthetic chemistry, various material and device characterization methods, device engineering. In order to fulfill the demand for the expertise necessary to appropriately address the organic electronics-related scientific topics, the research projects are often conducted in co-operations between various research groups. Since organic electronics has a potential to provide substantial revenues in the near future, electronic and chemical industries also show increasing interest in this field. As an outcome of this interest a significant research effort is also undertaken by industrial research and development (R&D) laboratories.

For the development of new organic electronic applications and improvement of performance of the already existing prototype devices, materials with desired properties play an instrumental role. They are the key ingredients, which provide competing functionalities (e.g. flexibility, lightweight) to the electronic devices. One of the most advantageous features, associated however mostly with soluble organic materials, is their good processing ability. The various organic-based devices can be made by printing methods, *e.g.* inkjet, roll-to-roll, which simplifies and speeds up the production process. Consequently, it also greatly lowers the manufacturing costs, which are often regarded as the deciding factors for successful commercialization of the devices.

Some of the developed organic materials already exhibit properties enabling their use in the electronic devices. Though for many applications, available at this time materials, do not provide satisfactory device performance and operational stability. Now a day these

shortcomings definitely hinder the progress in commercialization of organic-based electronic devices. For the sustainable development of organic electronics in-depth knowledge and understanding of physical and chemical properties of organic materials is necessary. One of the biggest drawbacks of organics is its tendency for alternation of properties not only during operation of devices but even under ambient conditions (often referred to as ageing). This in-turn constitutes a significant problem that limits both shelf and operational lifetime of the devices. Since many organic electronic applications encompass several thin film layers made of organics, and often also inorganic materials, the understanding of interfaces is another important issue for the development of organic electronics.

Luminescent Metal Chelates attracted tremendous attention and numerous potential applications have been proposed. The choice of metal ions for EL chelates is limited to those metals which do not exhibit d-d transitions that may interfere with the luminescence of the ligand. Therefore, aluminium (III), boron (III), beryllium (II) and zinc (II) are ideal. Since beryllium (II), boron (III) and aluminium (III) has no 'd' electron and zinc (II) has a closed shell of 'd' electrons. The metal ions only serve a structural purpose by stabilizing a luminescent ligand. Small organo-metallic complexes of Zinc have high stability , high efficiency, longer life and are ideal for as emitter materials in OLEDs.

1.1 History of Organic semiconductor

With the invention of the transistor around the middle of the last century, inorganic semiconductors like Si or Ge began to take over the role as dominant material in electronics from the before prevailing metals. At the same time, the replacement of vacuum tube based electronics by solid state devices initiated a development which by the end of the 20th century has lead to the omnipresence of semiconductor microelectronics in our everyday life. Now at the beginning of the 21st century we are facing a new electronics revolution that has become possible due to the development and understanding of a new class of materials, commonly known as Organic Semiconductors.

The enormous progress in this field has been driven by the expectation to realize new applications, such as large area, flexible light sources and displays, low-cost printed integrated circuits or plastic solar cells from these materials. Strictly speaking organic semiconductors are not new. The first studies of the dark and photoconductivity of anthracene crystals (a prototype organic semiconductor) date back to the early 20th century . Later on, triggered by the discovery of electroluminescence in the 1960s**[1,2]** molecular crystals were intensely investigated by many researchers. These investigations could establish the basic processes involved in optical excitation and charge carrier transport**[3,4]** Nevertheless, in spite of the principal demonstration of an organic electroluminescent diode incorporating even an encapsulation similar to the ones used in nowadays commercial display applications **[5],** there were several draw-backs preventing practical use of these early devices. For example, neither high enough current densities and light output nor sufficient stability could be achieved. The main obstacles were the high operating voltage as a consequence of the crystal thickness in the micrometer to millimeter range together with the difficulties in scaling up crystal growth as well as preparing stable and sufficiently well-injecting contacts to them.

Since the 1970s the successful synthesis and controlled doping of conjugated polymers **[6]** established the second important class of organic semiconductors which was honored with the Nobel Prize in Chemistry in the year 2000. Together with organic photoconductors (molecularly doped polymers) these conducting poly- mers have initiated the first applications of organic materials as conductive coatings **[7]** or photoreceptors in electro photography. The interest in undoped organic semiconductors revived in the 1980s due to the demonstration of an efficient photovoltaic cell incorporating an organic hetero-junction of p- and n-conducting materials **[8]** as well as the first successful fabrication of thin film transistors from conjugated polymers and oligomers **[9-11].** The main impetus, however, came from the demonstration of high-performance electroluminescent diodes from vacuum-evaporated molecular films **[12,13]** and from conjugated polymers **[14,15].** Owing to the large efforts of both academic and industrial research laboratories during the last 15 years, organic light-emitting devices (OLEDs) have progressed rapidly and meanwhile lead to first commercial products incorporating OLED displays **[16].** Other

applications of organic semiconductors e.g. as logic circuits with organic field-effect transistors (OFETs) or organic photovoltaic cells (OPVCs) are expected to follow in the near future**[17].**

1.2 Organic semiconductor

Organic electronics, or plastic electronics, is a branch of electronics that deals with conductive organic molecules. This is as opposed to traditional electronics which relies on inorganic semiconductors such as copper or silicon. There are three major classes of conjugated organic materials: (a) organic charge-transfer complexes, (b) various conjugated polymers derived from polyacetylenes, polyphenylenes, polypyrroles and polyanilines, and (c) pentacene and sexithiophene of the small conjugated molecules or oligomers. Organic conductive materials are lighter and more tunable than inorganic conductors.

In addition, the flexibility of organic synthesis enables the formation of organic molecules with useful luminescent and conducting properties and thus their usage as materials in organic field-effect transistors (OFETs),organic light emitting diodes (OLEDs) and photovoltaic cells. However, in general, the organic conductive materials have a higher resistance and therefore conduct electricity poorly and inefficiently as compared to inorganic conductors.

Organic materials are composed mainly of carbon atoms. Other low atomic number atoms, like: oxygen, sulfur, are also common building elements. The electronic configuration of carbon atom allows it to form different hybridized orbitals, namely sp, sp^2 and sp^3, as the chemical bonding configuration. The electronic configuration of carbon atom consists of 2 electrons in core 1s level denoted as $1s^2$ and 4 valence electrons residing in 2s and 2p levels, which can be denoted as $2s^2$ and $2p^2$, respectively. In order to explain electronic configuration in different compounds involving carbon, the concept of hybridized orbitals is used. Hybridized orbitals are assumed to be mixtures of atomic orbital. The wave functions of the s and p atomic orbitals combine to form a new set of

equivalent hybrid orbital. New orbitals are linear combinations of atomic orbitals and the reason they form is to minimize the total energy of the formed compound. When one s orbital mixes with three p orbitals it yields four sp^3 type hybrid orbitals. Each of them consists of two lobes of different size. Four larger lobes are oriented towards the corners of a tetrahedron at angles of 109.5º. When carbon atoms are bonded in such a scheme each of them has four neighbors. This configuration can be found in diamond. Another type of hybridization is the one that involves only one s and two p atomic orbital's. The three hybrids are span in the plane and are oriented at angles of 120º to one another and contain one electron each. The remaining electron resides in unhybridized p orbital oriented perpendicular to the plane of sp^2 orbitals In that case only one s and one p electrons form hybrid orbital. The remaining two p electrons are unhybridized and reside in orbitals oriented at 90º to the sp hybrids. Such hybridization scheme accounts for linear geometries.

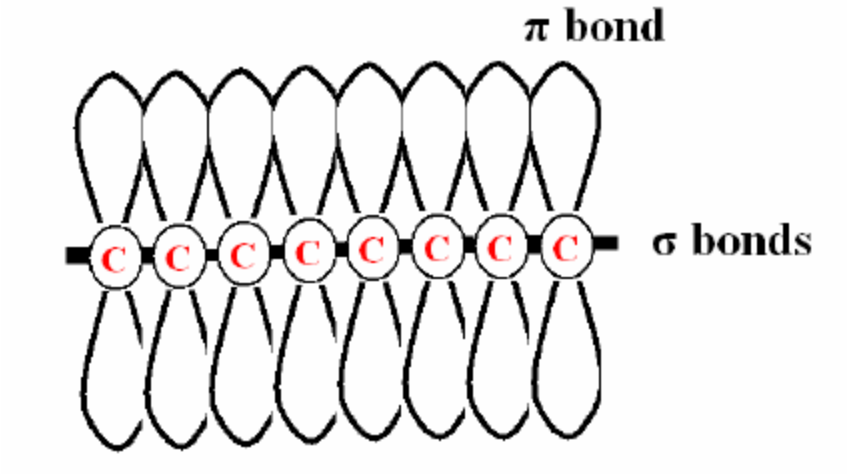

Figure 1.1: Schematic representation of σ and π bond in organic materials.

When two atoms are bond through hybridized orbitals, two different types of bond exist, depending on their alignment with respect to the bonding direction. Sigma bonds, denoted as σ, are symmetrical about the axis joining the two nuclei. This type of bond allows for rotation of atoms along the bonding direction. Most often such rotation is prevented by existence of π bonding. This bonding is constructed from electrons in unhybridized p orbitals and geometrically is perpendicular to the axis joining two nuclei.

Hence, when two carbon atoms are bonded through σ and π bonds, the later prevent rotation of these two atoms. These two types of bonds differ significantly by means of their strength. Since the spatial overlap of orbitals is larger for σ type of bonding than π type, the later is significantly weaker. This invokes consequences for the energy associated with σ or π electronic levels in a molecule (or bands in a polymer). The general picture in both cases is such that σ states are always lower in energy than π states (and *vice versa* for the occupied states). The existence of a single, double or triple bonds corresponds directly to the type of hybridization occurring when a molecule or polymer is formed. Another consequence of different hybridization schemes is the geometry of a compound. Polymers can be formed through sp^3 or sp^2 hybridization, which determines their electronic properties. Polymers with a backbone build from sp^3 hybridized carbon atoms have large band gap (above 3eV), which implies optical transparency and insulating properties. Units in such polymers are connected only through σ bonds. Another class of polymers often referred as conjugated polymers have their backbone build through sp^2 hybridization. In such configuration both σ and π bonds are present(Figure 1.1). The later are responsible for unique electronic properties of such systems.

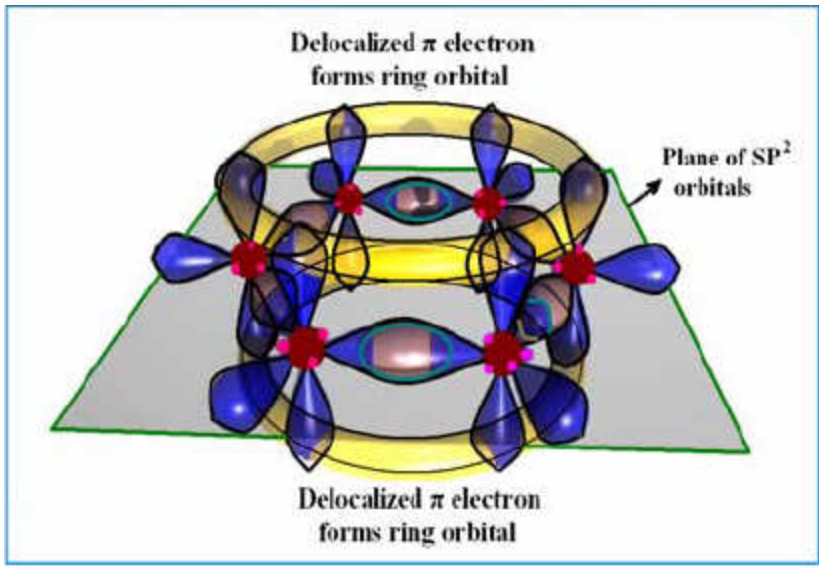

Figure 1.2: The π electrons of a benzene molecule form a delocalized ring orbital above and below the plane of the hexagon defined by the six carbon atoms.

Since there is interaction between π bonds of carbon atoms, the electronic wave function is delocalized along the polymer chain. This delocalization enables fast movement of charge-carrying species (polarons/bipolarons) along the backbone. As mentioned above, there are two major classes of organic semiconductors: now molecular weight materials and polymers. An important difference between the two classes of materials lies in the way how they are processed to form thin films. Whereas small molecules are usually deposited from the gas phase by sublimation or evaporation, conjugated polymers can only be processed from solution e.g. by spin-coating or printing techniques. Additionally, a number of low-molecular materials can be grown as single crystals allowing intrinsic electronic properties to be studied on such model systems **[18,19].** The controlled growth of highly ordered thin films either by vacuum deposition or solution processing is still subject of ongoing research, but will be crucial for many applications **[20].**

1.3 Organic light emitting diodes: structure and operation

Semiconducting polymers play a major role these days as active materials in a new generation of electronic and optical devices, including OLEDs **[21-23]** photo detectors, photovoltaic cells, solar cell, sensors**[24,25,26]** thin film transistors **[27-29]** and optical amplifiers/lasers. OLEDs are being considered for LCDs as one of the most promising next generation flat-panel displays because of their ease of manufacturing, all solid state design, and being self-emitting with wider viewing angle.

1.3.1 Structure/Fabrication of OLEDs

A typical OLED utilizes ~100 nm of a polymer/small molecule film sandwiched between an anode and a metal cathode. When a forward bias is applied, electrons are injected from the cathode into the LUMO of the polymer and holes are injected from the anode into the HOMO of the polymer. After carriers are injected, they drift in the presence of the externally applied electric field by hopping from molecule to molecule or through the polymer chain to the opposite electrode. A schematic structure of an OLED is shown in Figure 1.3.

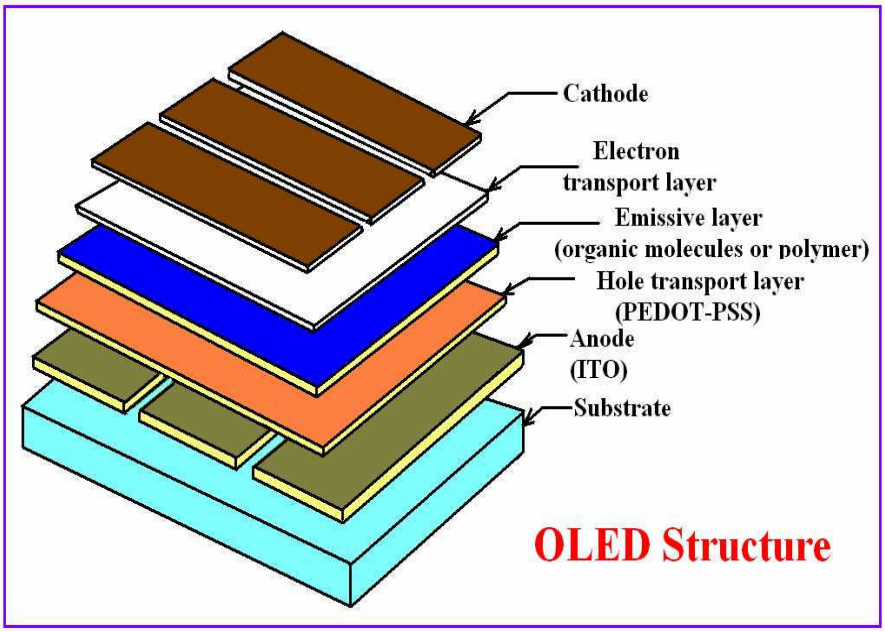

Figure 1.3: Schematic of the structure of a polymer/organic LED

Cathode may or may not be transparent depending on the type of metal used. The cathode is typically low-to-medium work function metal such as Ca (Φ = 2.87 eV), Al (Φ = 4.3 eV) or $Mg_{0.9}$ $Ag_{0.1}$ (Mg Φ=3.66eV) deposited either by thermal or e-beam evaporation. However, in case of Al and Ca, addition of an appropriate buffer layer (electron transport layer) between the top organic layer and the metal cathode improves the device performance considerably. Figure 1.4 shows a typical multilayer OLED structure. Appropriate multilayer structures typically enhance the performance of devices by lowering the barrier for hole injection from the anode and by enabling control over the e^- (electron) and h^+ (hole) recombination region, e.g., moving it from the organic/cathode interface, where the defect density is high, into the bulk. Hence the layer deposited on the anode would generally be a good hole transport material, providing the hole transport layer (HTL). Similarly, the organic layer in contact with the cathode would be the optimized electron transport layer (ETL**) [30].**

The existing OLED fabrication procedures fall into two major categories: (1) thermal vacuum evaporation of the organic layers in small molecular OLEDs (also known as SMOLED) and (2) wet coating techniques of the polymer layers. Thermal evaporation of small molecules is usually performed in vacuum of ~ 10^{-6} torr or better.

However it has been observed that the residual gases in the chamber may affect the performance of the device significantly. One of the most salient advantages of thermal vacuum evaporation is that it enables the fabrication of multilayer devices in which the thickness of each layer can be controlled easily, in contrast to wet coating techniques like spin coating. More about fabrication technique can be found in reference **[30].**

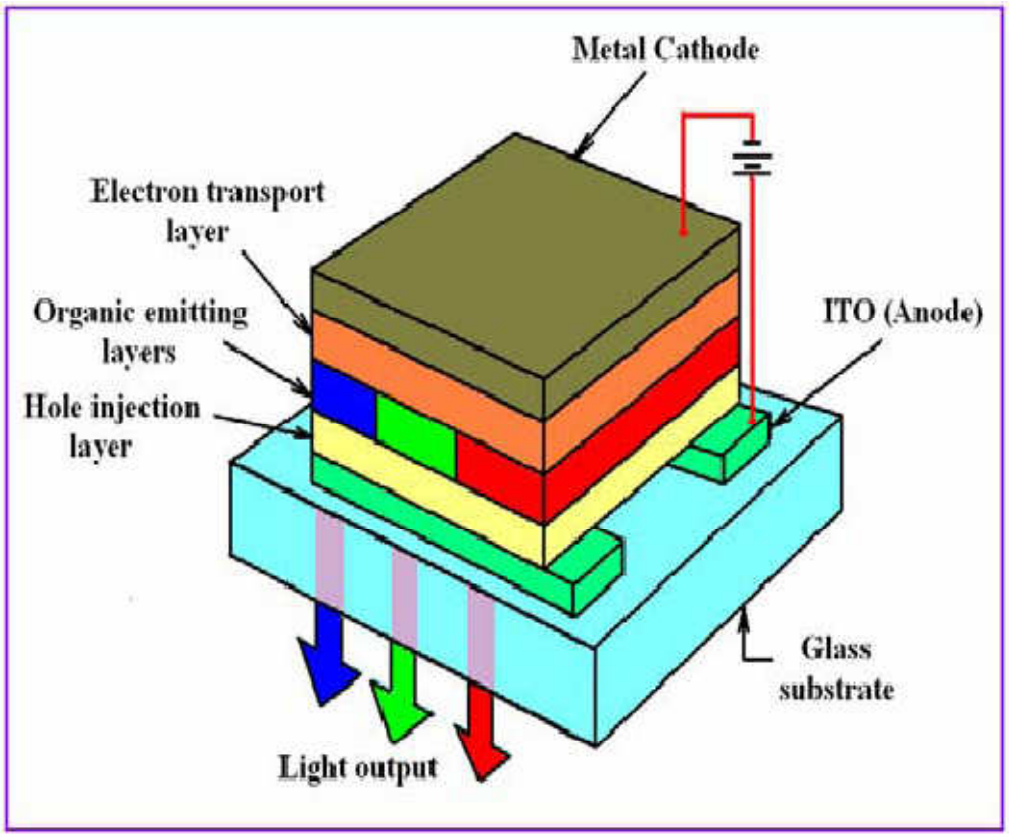

Figure 1.4: A typical multilayer OLED structure

1.3.2 Basic principle of OLED

Electrically injected carriers in an OLED recombine to generate light. The device physics is best illustrated by examining the simplest type of OLED with only a single organic layer. When an electron and hole capture one another within the organic layer, they form a neutral “exciton”, which is a bound excited state that can decay by emitting a photon **[31].** Schematic of the basic operation of OLED is shown in Figure 1.5 and the

step by step mechanism of generation of light in a typical OLED structure is shown in Figure 1.6.

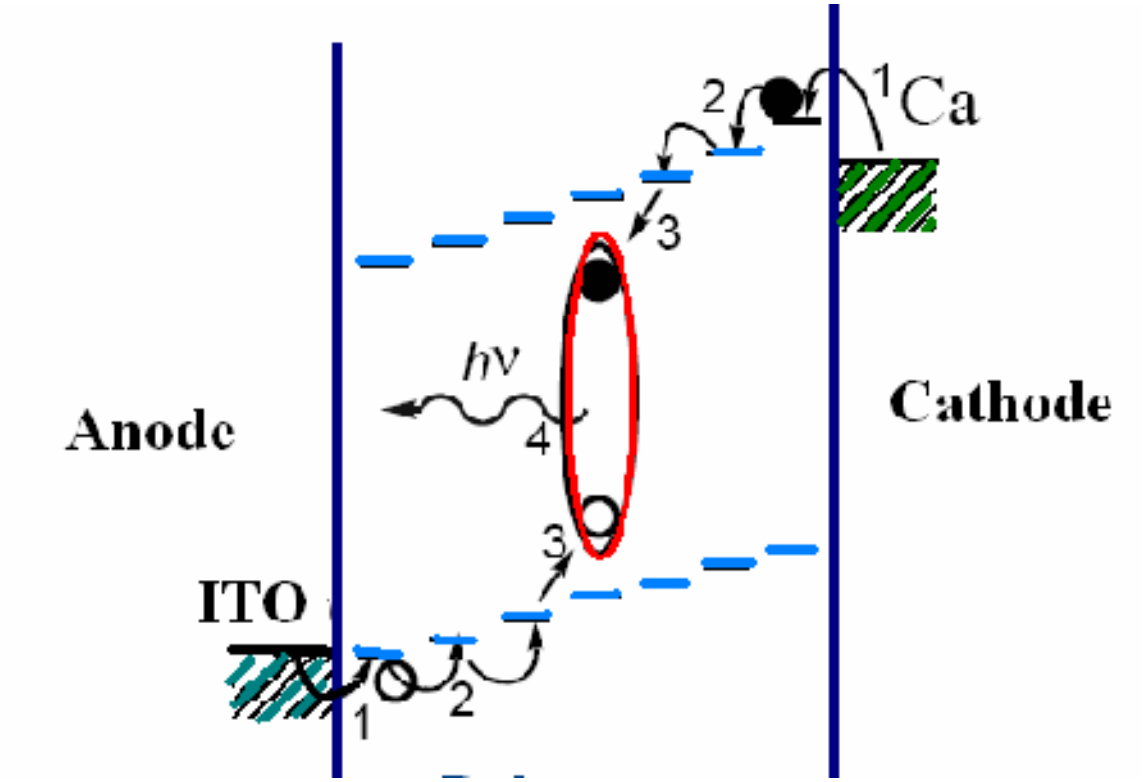

Figure 1.5: Basics of OLED. (1) Charge injection (2) Charge transport (3) Exciton formation (4) Light emission.

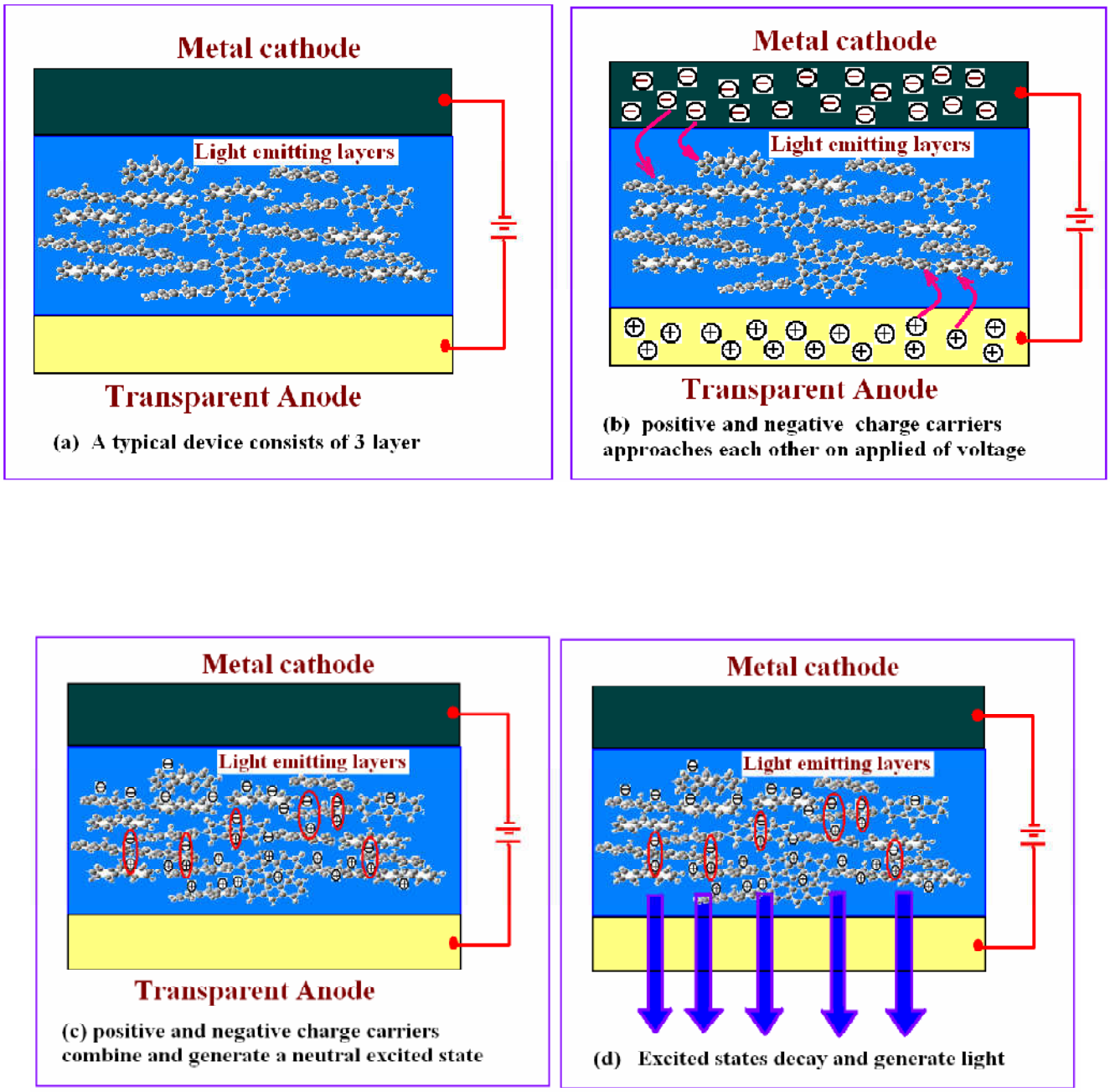

Figure 1.6: Step by step mechanism of generation of light in a typical OLED structure

1.3.3 Device Efficiency

The efficiency **[32]** of OLEDs can be characterized by its

- Quantum efficiency,
- Power efficiency (lm/W),
- Luminous efficiency (cd/A), sometimes called luminous yield.

1.3.3.1 Quantum efficiency

The device quantum efficiency η_q has two parts: internal and external:

(I) Internal quantum efficiency η_{int} or IQE is the number of photons generated inside the device per number of injected hole – electron pairs. A large fraction of generated photons stays trapped and absorbed inside the device.

(II)External quantum efficiency η_{ext} or EQE, is the number of photons released from the device per number of injected hole – electron pairs.

1.3.3.2 Power efficiency (lm/W)

Power efficiency η_p is the ratio of the lumen output to the input electrical watts (lm/W)

1.3.3.3 Luminous efficiency (Current efficiency) (cd/A)

Luminous efficacy η_v represents the ratio of the lumen output to the optical watts (radiative power). The luminous efficiency and luminous efficacy of a device account for a spectral sensitivity of a human eye. Therefore, two devices with similar quantum efficiencies can have different luminous performance, depending on the spectrum of the emitted light. In the process of converting electrical power into optical power, losses are incurred due to non-radiative processes (thermal relaxation of excitons, internal reflection and absorption of photons).

1.4 Carrier injection and transport in Organic semiconductor

All of the molecular materials used for Organic devices behave electrically as an insulator under the conditions of a low electric field ($<10^4$ V/cm). Typical vacuum-sublimed organic films showed a resistivity of the order of 10^{15} Ω-cm, which indicate that purified organic materials posses no net charge carriers intrinsically without chemical doping of donor and acceptor molecules. However, very high current density up to 1A/cm^2 in OLED can be obtained in operation. This fact is contradictory to the knowledge of organic semiconductors and new mechanisms were introduced for the explanation of the high current densities: carrier injection at electrode/organic interface, space charge limit current (SCLC) and trap charge limit current (TCLC). The large current density is provided by a carrier injection at an electrode/organic interface and SCLC. The electronic structure of organic thin films is based on the HOMO (highest occupied molecular orbital) and the LUMO (lowest unoccupied molecular orbital) of individual molecules. Each molecule interacts with a weak Van der Waals's force and forms narrow conduction and valence bands. The intrinsic carrier densities of organic semiconductors based on unavoidable impurities and irregular structures of thin films are very low, typically 10^5-10^{10}/cm^3. Also, a typical mobility of organic semiconductors is fairly small, 10^{-3}-10^{-7} cm^2/V-s, compared with that of inorganic materials, 1-10^3 cm^2/V-s. Carriers are injected into organics via Schottky thermal injection and Fowler- Nordheim tunneling injection.

1.4.1 Schottky thermal injection and Fowler-Nordheim tunneling injection

At the typical organic/electrode interface like Alq3/Mg , the energy barrier is about to be 1.0 eV, which is too high to generate any high current density. One of the possible injection mechanisms (Schottky thermal injection) is through the localized levels induced by structural defects and unexpected impurities. When a contact between the electrode and the organic layer is established, the image force potential is formed due to Coulomb attraction between the electrons injected and the holes left behind in the metal after the electron injection. The image potential lowers the energy of the interface state and makes them energetically available for the electrons hopping from the metal Fermi surface.

However, the image force potential decreases with increasing distance from the interface and thus the bulk states deep in the organic layer remain energetically unavailable for charge hopping. Application of an external field lowers the energy of the available states in the bulk of the organic layers. As a result, hopping into bulk states away from the interface becomes more probable. Another possibility of describing carrier injection is by Fowler-Nordheim tunneling injection. Electrons on the metal Fermi state can penetrate through the thin triangular energy barrier and hop into the energetically available state in the bulk. These two mechanism are illustrated below Figure 1.7(a) and (b). In both, the current injected is roughly exponential with T and applied field.

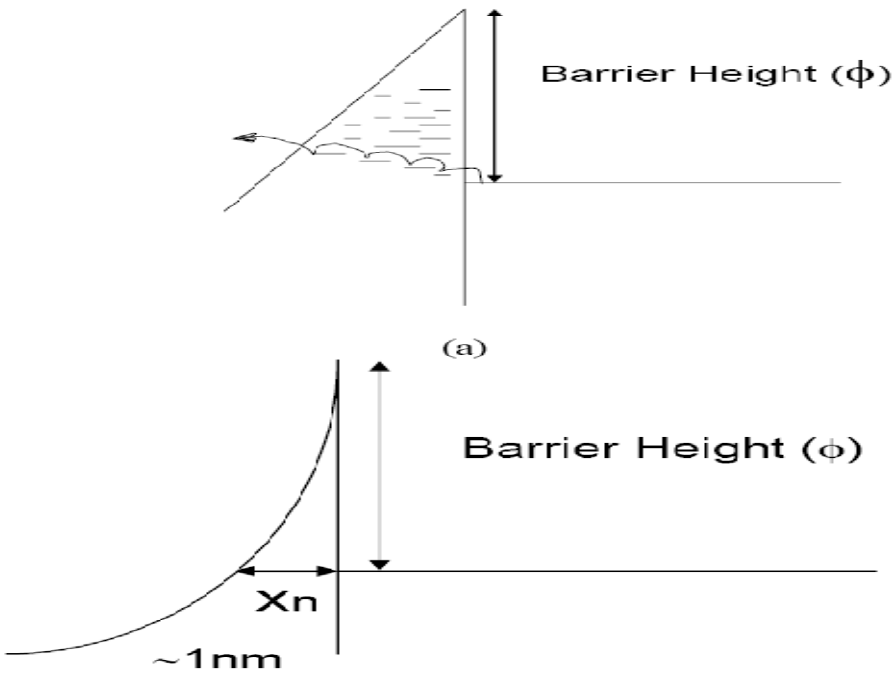

(b)

Figure 1.7: Two possible carrier injection mechanisms at the organic/metal electrode interface (a) Schottky-type carrier injection via impurity or structural disordered levels, (b) Fowler-Nordheim tunneling.

The Schottky emission process **[33]** is described by

$$J = \frac{4\pi qmk}{h^3} T^2 \exp(-\frac{q\phi}{kT}) \exp(\frac{qV}{kT} - 1) \quad \text{----------1.1}$$

Where m is the effective mass of the electron (hole); k is Boltzmann's constant, h is Planck's constant, T is the temperature, q is the elementary charge, φ is the barrier height, and V is the applied voltage.

For the Fowler-Nordheim tunneling injection, the current flow can be described by:

$$J = \frac{q^3 V^2 m_0}{8\pi h\phi m^*} \exp(-4\frac{(2m^*)^{0.5}\phi^{1.5}}{3hqV}) \quad \text{----------1.2}$$

Where m_0 is the mass of the free electron and m* is the effective mass.

1.4.2 Space charge limited current

When the applied electric field is less than 10^4 V/cm, injected current density is less than intrinsic charge density; the current flow is governed by Ohm's law. Mobility in organic luminescent materials are low. Charge injection into low mobility organic materials inevitably leads to charge accumulations in the organic film. This charge buildup partially screens out the applied electric field, leading to its redistribution. With the application of high external field (>10^5 V/cm), the injected current density is higher than intrinsic charge density near the electrode/organic interface because of low carrier mobility. Thus, the internal electric field is enhanced by the space charges and the current density J is governed by the SCLC **[34]** and can be described by

$$J = \frac{9}{8}(\frac{\varepsilon\varepsilon_0\mu V^2}{L^3} \quad \text{----------1.3}$$

Where ε is the relative dielectric constant, ε_0 is the dielectric constant and L is the sample thickness and μ is the field independent charge carrier mobility. The I-V curves predicted by this model are supralinear, typically quadratic in the absence of traps or with a single shallow trap level. Unlike inorganic semiconductors, the transport and the injection properties in OLEDs are determined by inter site hopping of charge carriers between localized states as well as hopping from delocalized states in the metal to localized states in the organic layer. The actual transition rate from one site to another depends on their energy difference and on the distance between them. The energy states involved in the hopping transport of holes and electrons form narrow bands around the HOMO and LUMO levels. The widths of these bands are determined by the intermolecular interactions and by the level of disorder. The space charge limited conduction (SCLC) type mechanisms are invariably found to dominate the conduction in device where strong injection is achieved from both electrodes. When an external electric field is applied, the holes are injected from the anode into the hole transporting layer (HTL) and drift or hop across it. However, they decelerate at the internal interface due to the lower hole mobility in the electron transporting layer (ETL). The same mechanism should also be true for electrons as they cross the organic/organic interface **[35],** which leads to substantial charge accumulation at the interface. If considering the carrier mobility is field dependent, the mobility can be described by a Poole-Frenkel**[36]** like equation:

$$\mu = \mu_0 \exp(\beta\sqrt{F}) \qquad \text{----------1.4}$$

Where μ_0 is the zero field mobility, β is an empirically determined coefficient and F is the external electric field.

1.4.3 Trap charge limited current

In addition to charges being localized to individual molecules, they can also accumulate in traps, typically at organic layer interfaces or at defects within the film. The local increase in the quasi-Fermi level due to strong injection my lead to charge immobilization in the deep states of the disorder induced distribution of the Highest Occupied Molecular Orbital (HOMO) and Lowest Unoccupied Molecular Orbital (LUMO)

levels. In that case, the resulting trapped charge limited current (TCLC) model predicts a generally high exponent power law**[35].** In the presence of traps, as the forward bias is increased, the electron quasi-Fermi level En rise towards the LUMO with increasing injected electron density. If traps are distributed in energy, they will be gradually filled with increasing field and the current will increase faster than quadratic in SCLC until all traps are filled. This model is called trap charge limited current (TCLC), in which a high power law dependence of current on voltage is observed. The trap energy can be described as exponentially distributed on the band gap by the equation

$$N_t(E) = \frac{N_t}{kT_t}\exp(\frac{E - E_{LUMO}}{kT_t} \quad \text{----------1.5}$$

Where N_t is the total trap density , k is Boltzmann's constant and T_t is the characteristic temperature of the exponential trap distribution ($T_t = E_t/k$, where E_t is the characteristic trap energy). Therefore, in the condition of high injection currents, the filling of traps below the quasi-Fermi level results in the current governed by the density and energy distribution of the traps. The current density then can be described as

$$J_{TCL} \sim V^{m+1}/d^{2m+1} \quad \text{----------1.6}$$

Where $m=T_t/T$.

1.4.4 Temperature dependence of carrier injection and transport

The carrier injection and transport show the temperature dependence which can be described by the equation (1.1)-(1.6). For the carriers injections from electrodes, the strong temperature dependence results from the thermal activation energy involved. For the carriers transport, temperature dependence of carriers mobility and trap energy distribution lead to the temperature dependent behavior. Although no widely recognized theory

regarding temperature dependence of the carriers behavior in real working devices has been proposed, some investigation show the temperature dependent I-V characteristics based on the temperature dependence of trap energy distribution, and the discrepancy between the temperature dependent mobility of carriers in OLED and semiconductor**.** Since the hole mobility in small molecule organic materials usually is much lower compared to electron mobility, the accumulation of holes at the HTL/ETL interface is very obvious. And the hole density at the interface shows strong temperature dependence, which will result in subsequent temperature dependence of charge balance factor **[35].**

1.5 The role of interfaces for charge injection

The electronic level alignment at the interfaces sets the conditions for the injection of charges in a device like e.g. OLED. Often, in organic diodes there are electronic level misalignments at the interfaces, which lead to the contact-limited injection regime. There are mainly two reasons for this situation. First of them is the mismatch between work function of the electrode and ionization potential (electron affinity) of the material in organic film, as shown in Figure 1.8. Another is the presence of additional barriers between organic layers *e.g.* HTL and active layer.

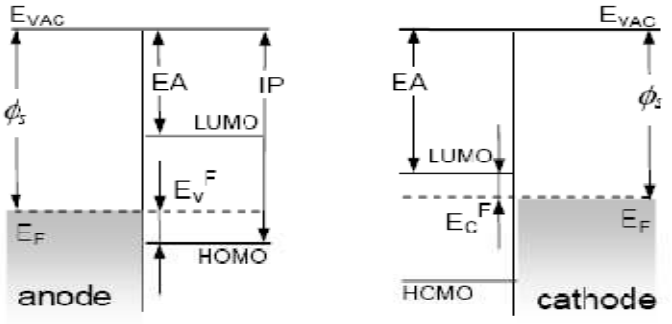

Figure 1.8: The schematic picture showing the energy level alignment at the interface of an electrode and organic layer. In these cases vacuum level alignment is assumed.

In both cases presented in Figure 1.8, a common vacuum level is assumed. The position of Fermi level versus vacuum level is given by the work function Φ_s of anode (cathode). Work function can be easily obtained by photoelectron spectroscopy as well as the threshold ionization potential (IP) of a molecule. In this way the hole-injection barrier can be estimated. In the case of electron injection barrier information of un-occupied states is needed, which can be provided by inverse photoemission spectroscopy. On this example, one can deduce that in order to obtain possibly barrier-less injection across the interface, the magnitude of the work function of an electrode should be (if possible) equal IP of organic material (or electron affinity (EA) in the case electron injection).

In the case of many heterojunctions, which involve inorganic electrode and organic materials, the assumption of common vacuum level is often not valid. Due to formation of chemical bonds, charge transfer or a "push-back effect", the interfacial dipole is formed, which manifests itself as a vacuum level offset (denoted as Δ)[**37-45].** As shown in Figure 1.9, such offset influences the magnitude of the barrier. In some cases, even when the work function of the substrate Φ_s equals ionization potential (IP) or electron affinity (EA) of organic material, there is still a barrier at the interface as the result of the vacuum level shift.

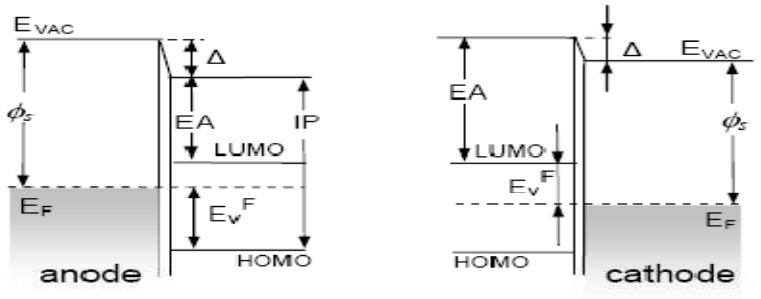

Figure 1.9: Schematic picture showing the energy level alignment at the interface of an electrode and organic layer. In these cases vacuum level shift is present, which increases injection barriers.

Therefore, the benefit of a good match between electrode work function Φ_S and the ionization potential (IP) of an hole transport layer (HTL), may be reduced by a negative

vacuum level shift that occurs at the corresponding interface. Such shift pushes molecular (or polymeric) electronic levels away from the substrate Fermi level. This effect seems to occur mostly for the interfaces with reactive or high work function metal surfaces, *i.e.*, metals with large surface dipole contribution to the work function. The existence of the barrier at the interface has its impact on device characteristics. In general the large magnitude of the barrier implies smaller injection current at the given voltage. This, in turn requires higher voltage applied to the device in order to achieve the desired intensity of light. These reasons are the main factors determining large interest within science and industry to understand and possibly control energy level alignment at the interfaces.

There are several different approaches to engineer an interface of desired properties. First of all for anode side of the device, the electrode used is almost always ITO, which has relatively high work function but still lower than IP of the most of the HTLs**.[46]** Therefore various HTLs materials have been studied in order to provide the best match between energy levels**[47].** On the other hand, by the modification of the surface of ITO, the work function can be significantly increased **[48-54]**.The hole-injection barriers can be reduced by increasing the work function of a substrate only to certain point. As the work function of the substrate exceeds the energy of integer charge transfer state (ICTS), the interfacial dipole is formed. The magnitude of the dipole scales linearly with Φ_S, while at the same time the barriers for hole injection remain constant. Any further increase in Φ_S has little (if any) effect on the charge injection barrier, but results instead in an interfacial dipole layer.

CHAPTER-2

MOTIVATION AND SCOPE OF THESIS

2.0 Introduction

Organic semiconductors such as semiconducting polymers and organic molecules are gaining a lot of attention of scientific community due to versatility of its application in sensors**[55],** organic light emitting diodes**[56],** solar cells**[57]** and thin film transistors**[58].**OLED displays is of particular interest as it offers many advantages such as low operating voltage, low power consumption and high contrast etc. Organic molecules have been known to show electroluminescence (EL) since the early 1960**[59].** The electroluminescence was reported for small organic molecules and conjugated polymer polyphenylene vinylene (PPV) **[12,60]**. Small molecules like Alq_3 **[61]** have been the materials of choice for organic light emitting (OLED) because of their process ability, relatively high efficiency, and a wide range of color emission for full color display. The OLED devices differ in one aspect from common inorganic semiconductors LED, due to low carrier concentration in the transport layer, the current voltage characteristics of these devices are injection limited**[62,63].** The balance of electron and hole in the emissive region is very important for fabricating highly efficient OLED. Several investigations have been carried to fabricate efficient OLED devices **[64-67]**.

2.1 Motivation

The discovery of a novel green electroluminescence device using organic material as the emitting elements had taken place in 1987**[68]**. The device has a double layer structure of organic thin film and efficient injection of holes & electron is provided from indium- tin-oxide (ITO) and an alloyed Mg:Ag cathode.

Since after the initial discovery of EL from Poly-phenylene-vinylene(PPV) by Burrough et al. in 1990**[69]** considerable progress has been made in the field of organic light emitting diodes. Despite the enormous versatility for optoelectronic applications, some of the fundamental physics underlying the construction or optimization of practical devices based on these organic materials remains controversial or poorly understood. Conjugated Polymers and small molecules have key advantages over their conventional solid-state inorganic counterparts in terms of tunability of the emissive color by structural modifications. Band gap and color tuning of these materials by chemical modification and copolymerization offer extensive research work for high efficient Red-Green-Blue (RGB) LEDs, which constitute the active elements in a new generation of nanoscale plastic optoelectronic devices**[70,71].** In addition, structure, defect states and disorder impact the charge transport properties that eventually govern the performance of these devices.

Charge injection, charge transport, and recombination are the three crucial contributions that optimize the device efficiency of a polymer LED**[72].** An unbalanced injection results in an excess of one carrier type that does not contribute to light emission, which can rise to confinement of EL emission to a region close to one of the injecting electrodes, where enhancement of nonradiative decay rate is expected and thereby decrease the quantum efficiency substantially**[73].** The development of organic multi-layer structure considerably improved the efficiency of light-emission by achieving a better balance of the number of charge carrier of opposite sign and further lowered the operating voltage by reducing the mismatching of energy levels between the organic materials and the electrodes. The consequence of this development was the demonstration of organic light emitting devices(OLEDs) by Tang et.al with true potential for lighting and display applications**[12,13].**

The charge injection and transport at the organic–metal interface of the OLEDs have been extensively studied and reported **[74-76].** The classic mechanism of the charge carrier injection depends on the potential barrier at the interface and on the temperature

dependent energy of electrons and holes incident on that barrier**[77].** Therefore, for improving efficiency of OLED devices modification in the interfaces, understanding of charge injection and charge transport need to be investigated.

2.2 Scope of thesis

The charge injection, charge transport and various other modifications are necessary and important for improving the efficiency of OLED devices. Therefore,the studies of the present thesis are aimed at

1. Anode modification
2. Multi layer structure to increase the efficiency of OLED.
3. Synthesis of novel organic emissive material for OLED.
4. Study of temperature dependent transport properties of a small organic material for better transport of charge carrier.
5. Study of thickness dependent electrical transport properties.

CHAPTER -3

EXPERIMENTAL DETAILS

In this Chapter, the main organic materials used in this study will be introduced, which includes their molecular structures and relevant physical properties. Then, device preparation and characterizations will be presented.

3.0 Materials and their properties

Zn(HPB)mq and CuPc have been used in the present work. The method of synthesis and processing of these material have been discussed in subsequent section.

3.0.1 {(2-(2-hydroxyphenyl)benzoxazole)2-methyl -8-hydoxyquinoline}zinc [Zn(HPB)mq]

{(2-(2-hydroxyphenyl)benzoxazole)2-methyl -8-hydoxyquinoline} zinc [Zn(HPB)mq] was synthesized in a 100 ml round-bottomed flask, 2-(2-hydroxyphenyl) benzoxazole (HPB) (0.844gm) (Sigma Aldrich) was dissolved in 40 ml of anhydrous ethanol at 70 ^{0}C under a nitrogen atmosphere .The solution was stirred for 2h, after which 2-methyl -8-hydoxyquinoline(mq)(0.636gm) dissolved in 40ml of anhydrous ethanol was added drop wise while stirring continued for 2 h after which zinc acetate dihydrate (0.876 gm) in water (6 ml) was added drop wise to the reaction mixture while stirring continued. After 2 hrs of stirring a precipitate of the complex was separated, which was filtered and recrystallized from a mixture of acetone and ethanol and dried in a vacuum oven . The synthesized material was further purified by vacuum sublimation. In this study this material used as emissive material as well as electron transport material.

3.0.2 Copper Phthalocyanine (CuPc)

The phthalocyanines are a class of organic semiconductors which are chemically and thermally stable, and, thus, suitable for the preparation of thin film . They commonly

exist in at least two different crystalline phases, the α- and β- forms . It was reported that the β - form is a monoclinic crystal. Metal phthalocyanines (MePc) are macrocyclic metal complexes with 18-electrons in the macro cyclic ring and mostly used as dyes. MePc molecules consist of a fourfold π-conjugating macro cyclic ring in which four iso-indoline groups are bound by aza-nitrogens. A huge number of metal-phthalocyanines can be formed with same molecular structure(as shown in figure 3.0),which provides versatile and flexible chemical systems(central ion and substituent).

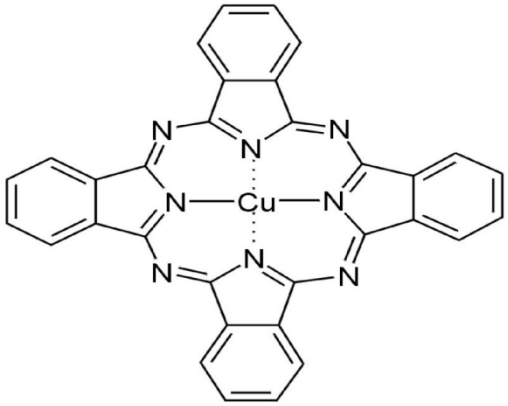

(a)

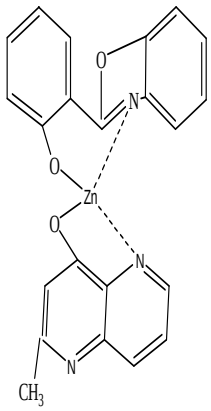

(b)

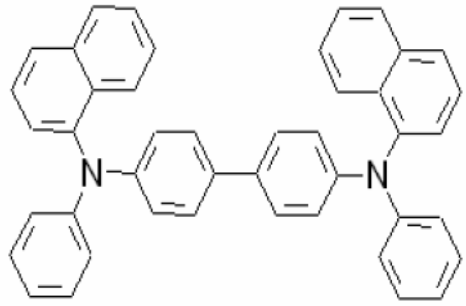

(c)

Figure: 3.0 Molecular structure of (a)CuPc (b)Zn(HPB)mq (c). α-NPD

3.0.3 Hole conduction materials for hole transport and electron blocking

A typical hole conduction material usually has a hole mobility several orders of magnitude higher than its electron mobility so that its electron transport ability can be neglected. Hole conduction materials were used in this study as matrix of the hole transport layer, as electron blocker. In this work N, N'-di(naphthalen-2-yl)-N, N'-diphenyl-benzidine (α-NPD) has been used as hole transport layer and electron blocker for OLED. . Other hole transporter material are 2,2',7,7'-tetrakis-(N,N-diphenylamino)-9,9´-spirobifluorene (Spiro-TAD), N,N,N',N'-tetrakis(4-methoxyphenyl)-benzidine (MeO-TPD),CuPc etc. The present study also includes CuPc as hole transport layer.

3.0.4 Electron conduction materials for electron transport and hole blocking

In contrast to hole conduction materials, an electron transport material has much smaller hole mobility compared to its electron mobility. They were used in this study as matrix of the electron transport layer and as the hole blocking layer. In this study Lithium Fluoride (LiF) is used as electron transporter and hole blocking material. Other electron transporter materials are 4,7-diphenyl-1,10-phenanthroline (Bphen) Bis(2-methyl-8-quinolinolato)-(para-phenylphenolato)-aluminium(III) (BAlq) .

3.1 Optical Characterization Techniques

The optical characterization technique used in present study includes UV-absorption and Photoluminescence spectroscopy. The details of these techniques are given in subsequent section.

3.1.1 UV-Visible Absorption Spectroscopy

The process of absorption is caused by the onset of optical transitions across the fundamental band gap of the material. When electrons are excited between the bands of a solid by making optical transitions that are dictated by selection rules it is called interband absorption**[78].**

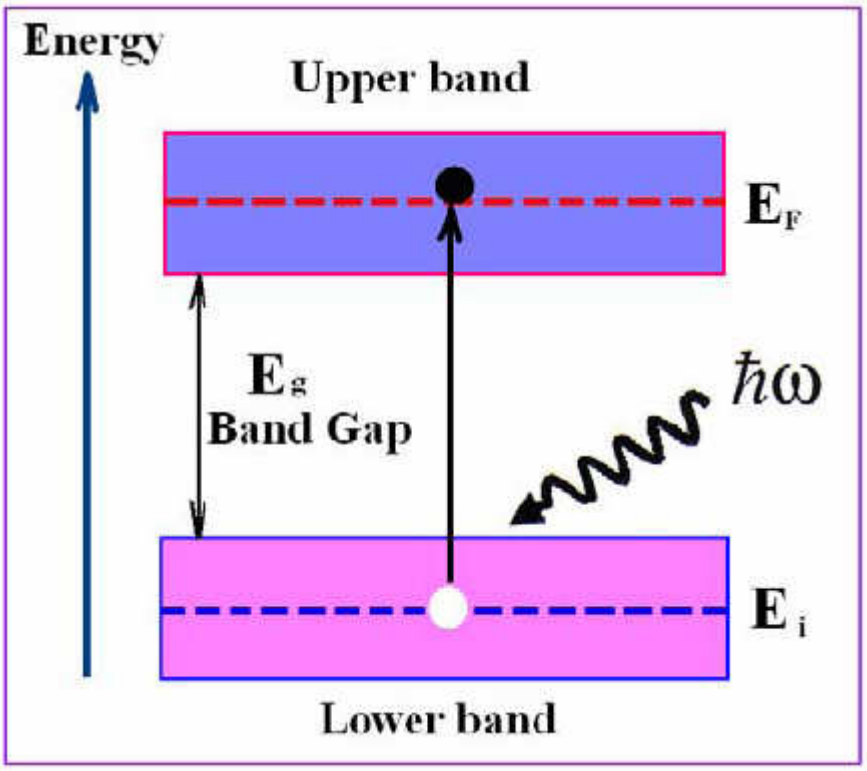

Figure 3.1: Interband optical absorption between an initial state of energy E_i in an occupied lower band and a final state at an energy E_f in an empty upper band. The energy difference between the two bands is the band gap [79].

An absorption spectrophotometer is an instrument that measures the amount of optical absorption in a material, as a function of wavelength. There are four main components of a spectrophotometer: (1) a light source which is usually a tungsten filament or gas-discharge lamp. Different light sources are used in different regions of the spectrum. (2) a monochromator ; the input to the monochromator is the broadband light from the light source; the output is tunable and highly monochromatic light. (3) a sample chamber which holds the sample under investigation, and (4) a detector which measures the amount of light that passes through the sample. Typically, detectors are either solidstate photodiodes (silicon, germanium, etc.) or photomultiplier tubes. The basic setup for measuring the absorption or transmission of light through a sample is shown in Figure 3.2.

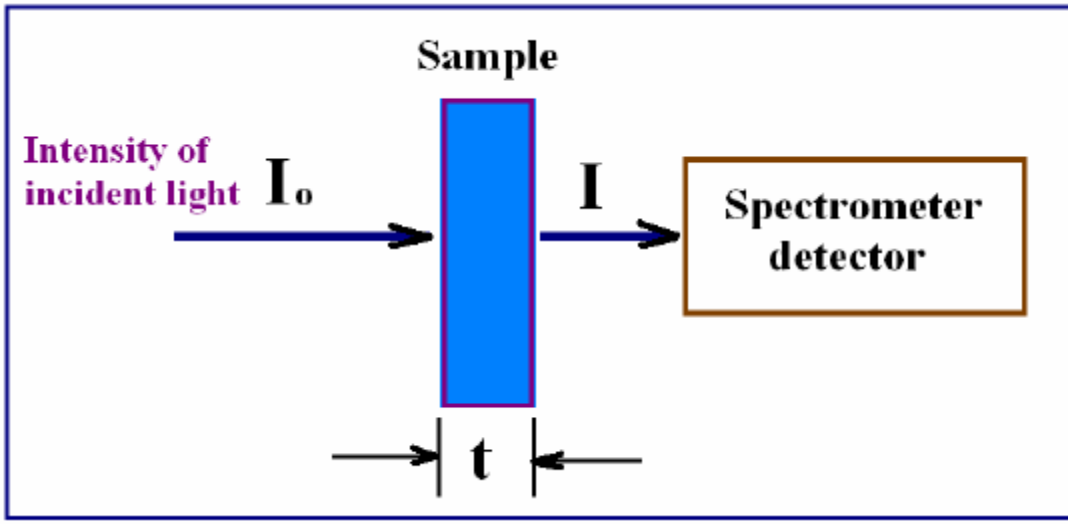

Figure 3.2: Light of intensity I_o incident upon a sample of thickness t undergoes a loss in intensity upon passing through the sample. The intensity measured after passing through the sample is I.

When light of some wavelength λ with intensity I_o passes through the sample the intensity of the light is reduced to a value I, due to absorption within the sample and reflection at the surfaces of the sample. Measuring I_o and I can be used to determine the transmission of the sample at wavelength λ. In addition to transmission, another useful way to report the optical absorption is in optical absorbance or optical density.

Absorbance (*A*) is a dimensionless quantity defined as the negative of the base-ten logarithm of the transmission (*T*) $A = -\log_{10}T$. Another quantity of interest is the absorption coefficient (α). The absorption coefficient is given by Beer's Law which relates I to Io by *t* $I = I_o e^{-\alpha t}$ where "*t* " is the thickness in cm and consequently, absorption coefficient α is in cm^{-1}. As the absorbance is the negative base-ten logarithm of the transmission then $\alpha = 2.303A/t$. Absorption spectrometers measure the intensity of the transmitted light as a function of wavelength and compare it to the intensity of the reference at the same wavelength **[78,79].**

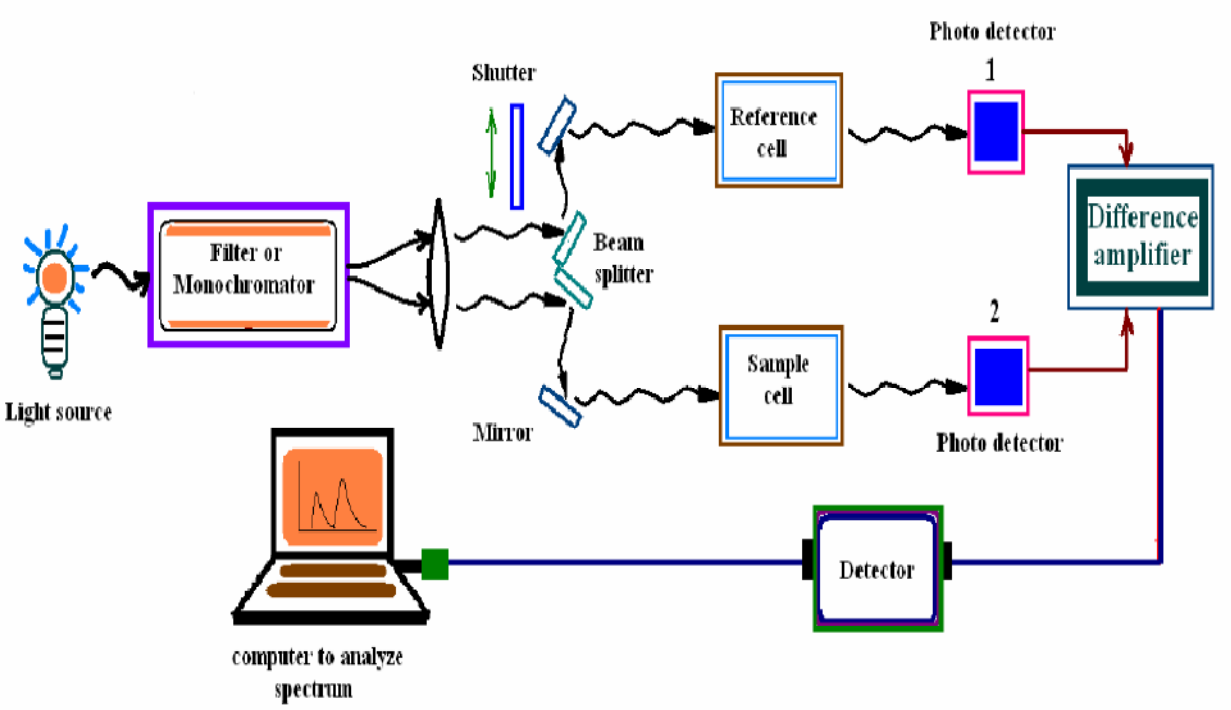

Figure 3.3: Schematic of double beam UV-Visible spectrometer to measure absorption spectra in the wave length range of 200 nm -900 nm.

For the experimental absorption spectra measurements of polymer, thin films were prepared by spin coating from toluene solution on to a sapphire substrate. The ultraviolet visible spectra (UV-Visible) absorption spectra were measured on a Shimadzu UV 2401 PC UV visible recording spectrometer. The schematic is shown in Figure 3.3.

3.1.2 Photoluminescence Spectroscopy

When light of sufficient energy is incident on a material, photons are absorbed and electronic excitations are created. Photo-excitation causes electrons within the material to move into permissible excited states. When these electrons return to their equilibrium states, the excess energy is released by emission of light (a radiative process) or via a nonradiative process. If radiative relaxation occurs, the emitted light is called photoluminescence (PL). The energy of the emitted light is related to the difference in

energy levels between the two electron states involved in the transition between the emitted states and excited states.

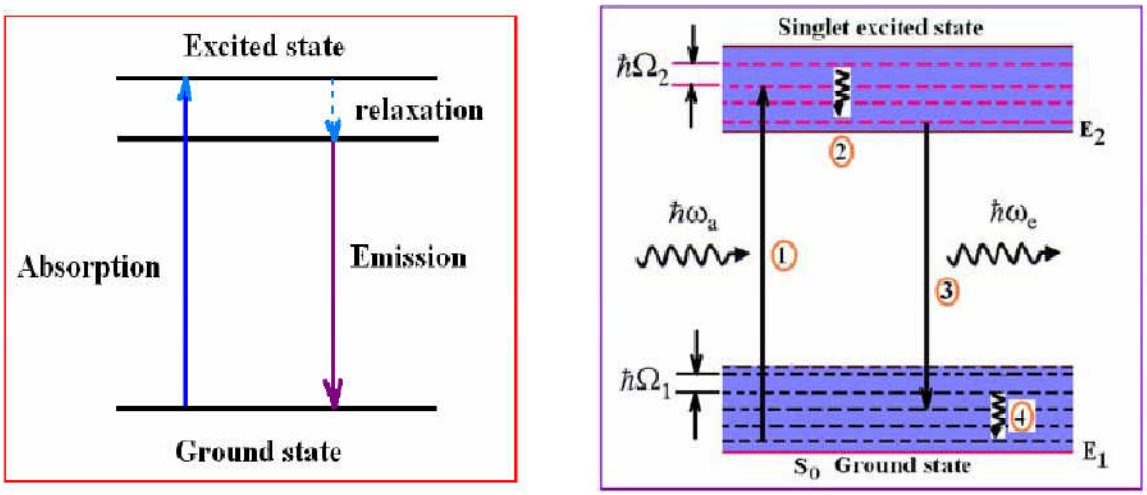

Figure 3.4 : (Left) Luminescence process and (Right) schematic diagram of the vibrational electronic transitions in a molecule between the ground state and an excited state (1) absoption (2) non-radiative relaxation (3) emission (4) non-radiative relaxation[79].

Photoluminescence(PL) is simple, versatile, and nondestructive. The instrumentation that is required for ordinary PL work is modest: an optical source (laser), mirror, collection lenses, optical power meter or spectrophotometer, and a photo detector. A typical PL set-up is shown in Figure 3.5.

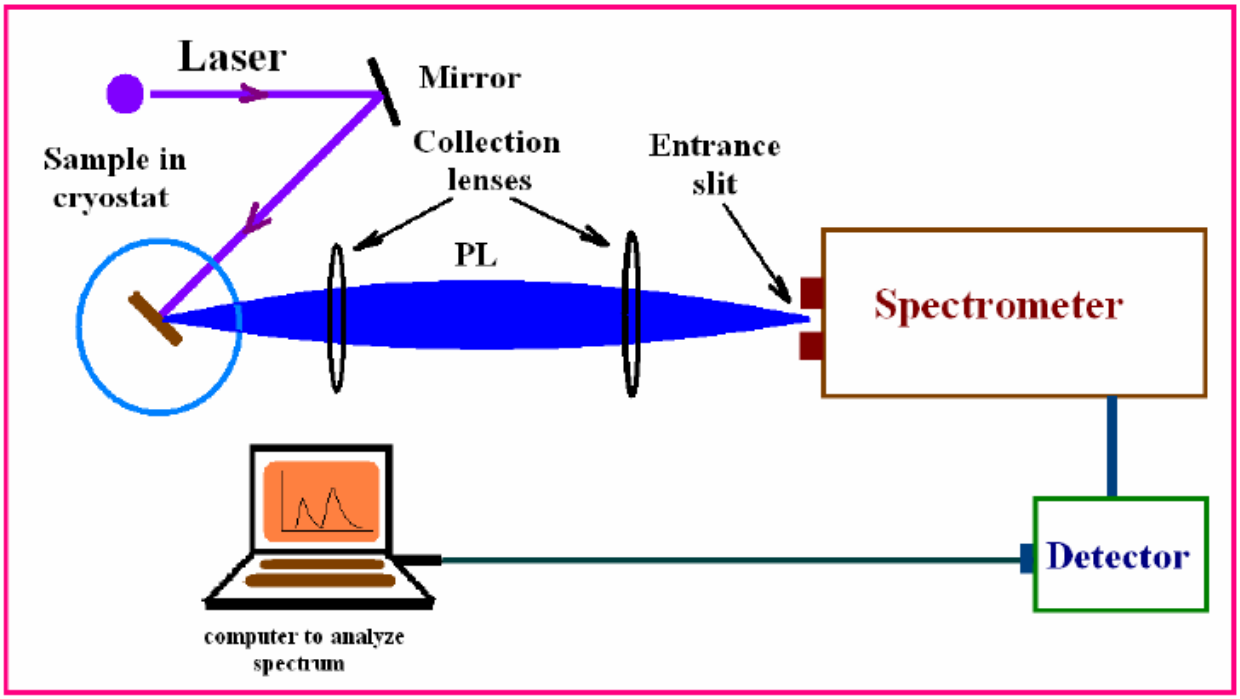

Figure 3.5: Typical schematic diagram and experimental setup for Photoluminescence measurements.

The UV line of an Ar^+ (argon ion) was used in our experiment. There are three lines of wavelength in UV laser 351.4 nm, 351.1 nm, and 363.8 nm respectively. An external prism was used to separate lines. Neutral density filters were used to reduce the intensity of the laser line to avoid heating the sample. The emission spectra were collected using a miniature flexible fiber optic spectrometer USB 2000 detector. For some measurements the 325 nm line of HeCd laser was also used as the excitation source. The schematic of our Photoluminescence system is shown in Figure 3.6.

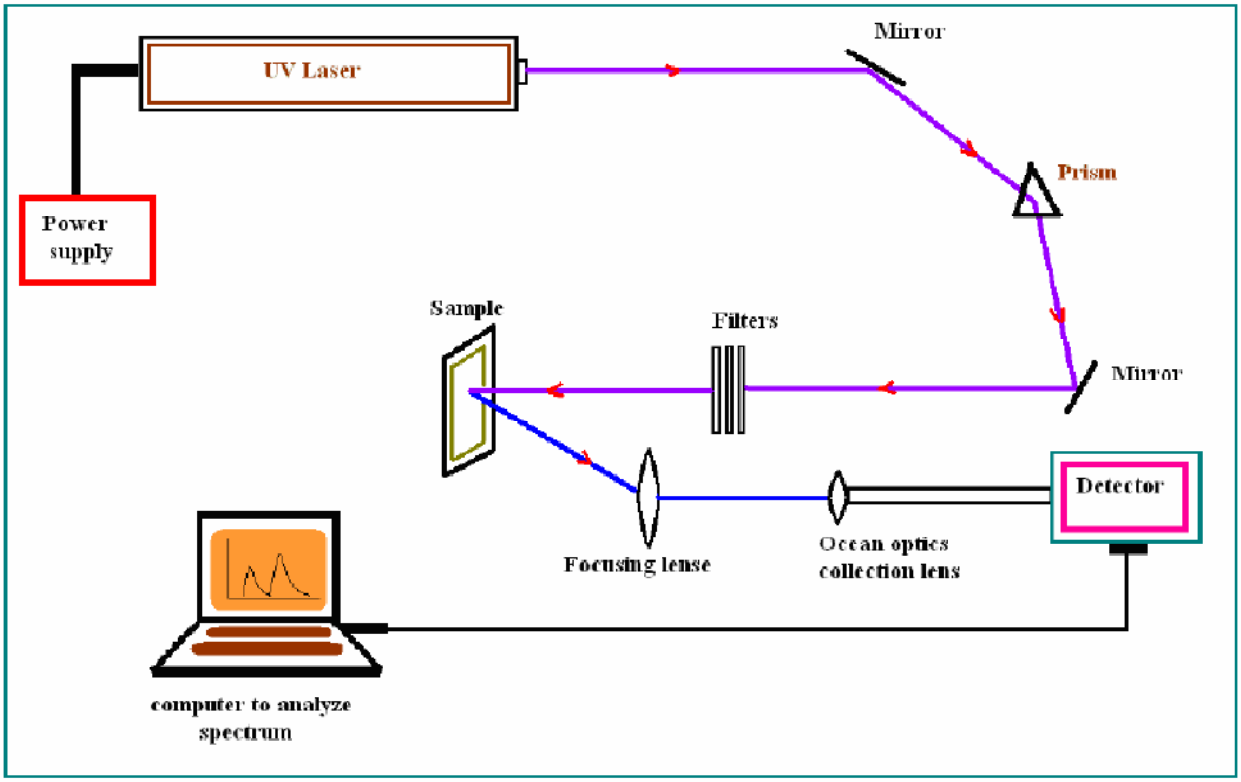

Figure 3.6: Schematic of the experimental arrangement used for the observation of photoluminescence spectra of PF and PF-based LED.

3.2 Thermo Gravimetric Analysis

Thermo Gravimetric Analysis (TGA) is a thermal analysis technique**[80]** used to measure changes in the weight (mass) of a sample as a function of temperature and/or time. TGA is commonly used to determine polymer degradation temperatures, residual solvent levels, absorbed moisture content, and the amount of inorganic (noncombustible) filler in polymer or composite material compositions. A simplified explanation of a TGA sample evaluation may be described as follows. A sample is placed into a tarred TGA sample pan which is attached to a sensitive microbalance assembly. The sample holder portion of the TGA balance assembly is subsequently placed into a high temperature furnace. The balance assembly measures the initial sample weight at room temperature and then continuously monitors changes in sample weight (losses or gains) as heat is

applied to the sample. TGA tests may be run in a heating mode at some controlled heating rate, or isothermally. Typical weight loss profiles are analyzed for the amount or percent of weight loss at any given temperature, the amount or percent of noncombusted residue at some final temperature, and the temperatures of various sample degradation processes.

3.3 Device Processing

3.3.1 Substrate Cleaning and Preparation

All substrates were cleaned and prepared prior to use. The preparation method depends on the substrate in question. Substrate cleaning involves the use of chemicals that pose significant health risks, therefore all procedures were performed in a fume hood or glove box while wearing appropriate personal protective equipment as outline on the material safety data sheets.

The plates of ITO coated glass 25 mm X 25 mm X 1.1 mm were patterned by placing strips of scotch tape at approximately 3 mm intervals. The substrate is coated with zinc powder and placed in a 37% HCl and distilled water bath. Through manual abrasion and chemical reaction the ITO in the exposed regions was removed. The etched sample was rinsed thoroughly with water and the tape removed leaving a patterned surface. Following patterning, the substrates were put into a clean teflon holder and sonicated in an acetone bath for 15 min. This was followed by 15 min of sonication in an isopropanol bath. The substrates were then rinsed with fresh isopropanol and blown dry with oil free nitrogen gas. Finally they were placed in an Ultra Violet Ozone Cleaning Systems for 10 min before being transferred to the glove box/thermal evaporation system for use or stored in a covered Petri dish for use clean substrates were essential for obtaining reliable and repeatable experimental data. Organic surface contaminants may react chemically with the polymer film or electrode material while metallic/insulating particles may contribute to unusual film morphology and device performance.

3.3.2 Device Fabrication Technique

Fabrications of a OLED includes the deposition of a thin film (polymer or small molecules) over a glass substrate which is already coated with Indium tin Oxide (ITO) which is the anode and a low work function metal is the cathode. Typically organic layer thickness is nearly 100 nm. A deposited thin film is a layer on a surface having properties that differ from those of the bulk material (substrate) that has been formed by the addition of solid materials to the surface. Generally, the substrate material cannot be detected in the film, which can be an organic or inorganic material. This surface layer differs from surface conversion where the surface is chemically converted to another material, e.g., anodization of aluminum. The term thin film is generally applied to layers that have thicknesses on the order of several micrometers or less. These films may be as thin as a few atomic layers. In many cases, adding atoms or molecules to a substrate surface one at a time forms thin films. Thicker layers are generally called coatings. Although the same processes that are used to form thin films can often form coatings, there are some coating processes that are not applicable to forming thin films. For example, thermal spray coating processes, which melt small particles, accelerate them to high velocities, and splat-cool them on the surfaces, are not applicable to forming thin films. The properties of thin films generally differ from the values for the materials in the bulk form. In many cases, the growth and properties of thin films are affected by the properties of the underlying substrate material. The properties of the film can also be affected by the high surface to volume ratio of the film. Many technique are used for device fabrication, one of them we used for device fabrication was vacuum evaporation technique. Before preparing a device its patterning is very important. To obtain desired patterns from OLEDs the layer of ITO on glass surface is shaped in a certain manner. It is achieved by Photolithography.

3.3.2.1 Vacuum Evaporation Techniques

Vacuum deposition, some time called vacuum evaporation technique, is a major physical deposition technique that is extensively used for the deposition of thin films on

the surface of a substrate. The vacuum thermal evaporation (Figure-3.7) deposition technique consists in heating until evaporation of the material to be deposited. The material vapor finally condenses in form of thin film on the cold substrate surface and on the vacuum chamber walls. Usually low pressures are used (about 10^{-6} or 10^{-5} Torr), to avoid reaction between the vapor and atmosphere. At these low pressures, the mean free path of vapor atoms is the same order as the vacuum chamber dimensions, so these particles travel in straight lines from the evaporation source towards the substrate. This originates 'shadowing' phenomena with 3D objects, especially in those regions not directly accessible from the evaporation source (crucible). Besides, in thermal evaporation techniques the average energy of vapor atoms reaching the substrate surface is generally low (i.e. kT, order of tenths of eV). This affects seriously the morphology of the films, often resulting in a porous and little adherent material. In thermal evaporation techniques, different methods can be applied to heat the material. The equipments available in the laboratory use either resistance heating (Joule effect) or bombardment with a high-energy electron beam, usually several KeV, from an electron beam gun (electron beam heating). The principal processing variables in vacuum deposition are deposition geometry, deposition rate, and substrate temperature during deposition and the level of gaseous and vapor (e.g., water vapor) contamination in the deposition environment.

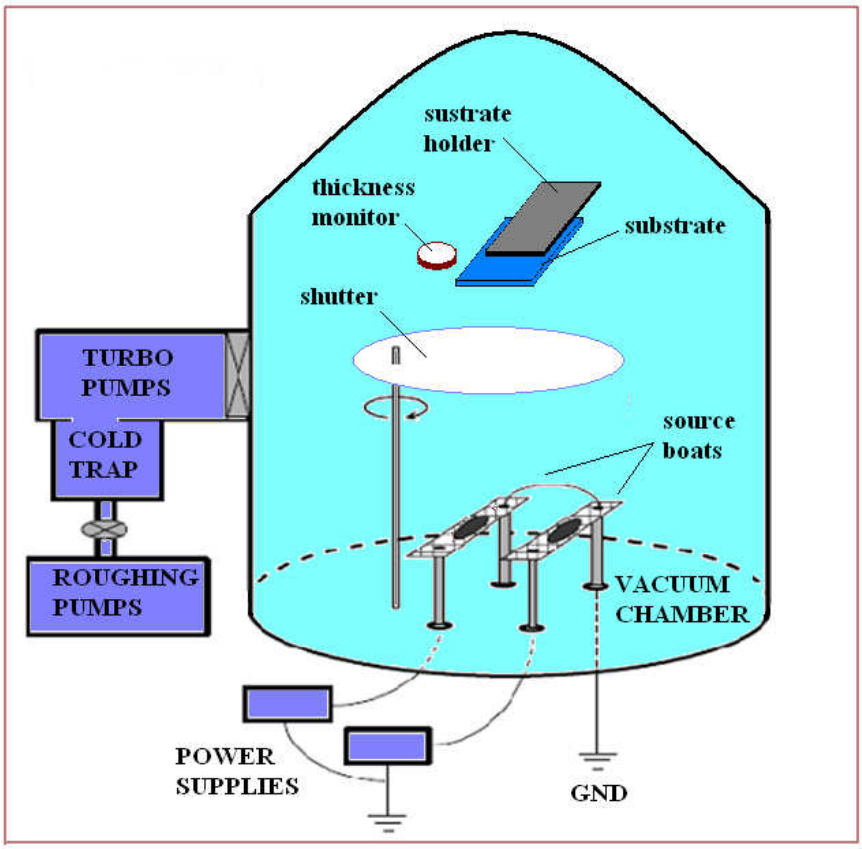

Figure 3.7: Thermal Vapour Evaporation Technique

Deposition rates and amounts can be monitored in situ and in real-time by oscillation frequency to change. Calibration allows the change in frequency to be related to deposited film mass and by assuming a film density, the film thickness. In many applications the amount of material deposited is controlled by the evaporation-to-completion of a specific amount of material and using specific deposition geometry. In many cases a property of thin film, such as optical transmittance, is monitored during deposition and is controlled the amount of material deposit.

3.3.3 Device Fabrication

3.3.3.1 Organic Light Emitting Diode

The OLED device was fabricated in a configuration ITO (120nm)/α-NPD (40 nm)/Zn(HPB)mq (35 nm/LiF(1 nm)/Al(300 nm)as shown in schematic diagram of OLED Device Figure 3.8 . Indium-tin oxide (ITO) coated glass substrates with sheet resistance

of 20 Ω/□ were patterned using photolitheography and cleaned using trichloroethylene, acetone, isopropyl alcohol and deionised water sequentially for 20 minutes using an ultrasonic bath and dried in flowing nitrogen. Prior to film deposition, the ITO substrates were treated with oxygen plasma for 5 minute. On the substrate, the hole transport layer and the emitting layers were deposited sequentially under a high vacuum (1×10^{-5} torr) at a deposition rate of 0.2 - 0.5 Å/sec and LiF at 0.1-0.2 Å/sec. Thickness of the deposited layers were controlled by a quartz crystal monitor. The cathode was deposited on the top of the structure through a shadow mask. A 40 nm N,N diphenyl-N'N'-bis(1- naphthyl)-1,1'-biphenyl-4,4'-diamine(α-NPD) (Sigma Aldrich) was used as hole transport layer. Zinc complex Zn(HPB)mq was used as the emitting layer . The electron injection was facilitated using a 1nm thin LiF (Merck, Germany) layer followed by a thick layer of Aluminium. The device area was 5 × 5 mm. The Luminance–Current–Voltage (I-V-L) characteristics were measured using a luminance meter (LMT 1009) and a Keithley 2400 programmable voltage-current digital source meter.

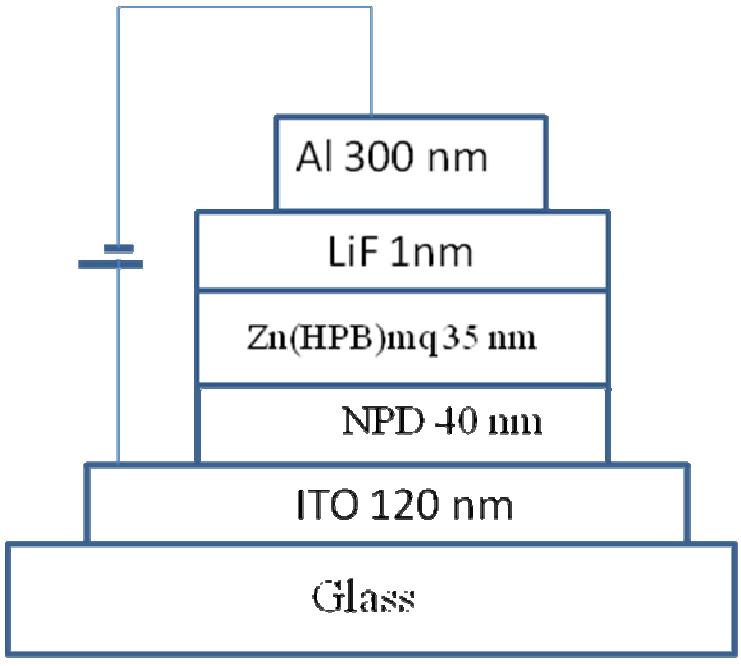

Figure3.8: Device Structure Fabricated For OLED

3.3.3.2 Transport measurement

The nature of the electrical transport mechanism for carrier transport in CuPc and Zn(HPB)mq has been studied by current-voltage measurement of samples at different temperatures. In this thesis work, hole transport behavior of CuPc single layer devices (ITO/CuPc/Al as shown in Figure 3.9) have been studied at different thickness and at different temperature and the electron transport behavior of Zn(HPB)mq single layer device (ITO/Zn(HPB)mq/Al as shown in Figure 3.10) has been studied at different temperature for thickness 200 nm.

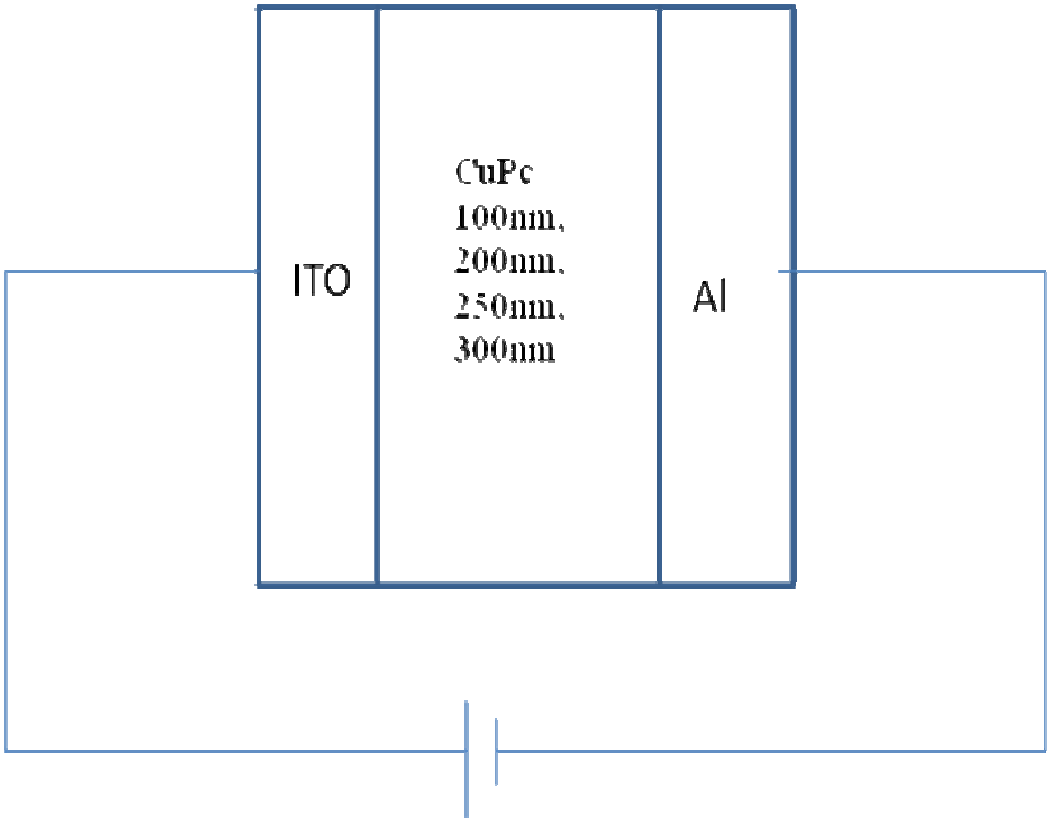

Figure 3.9: Hole only device for transport studies

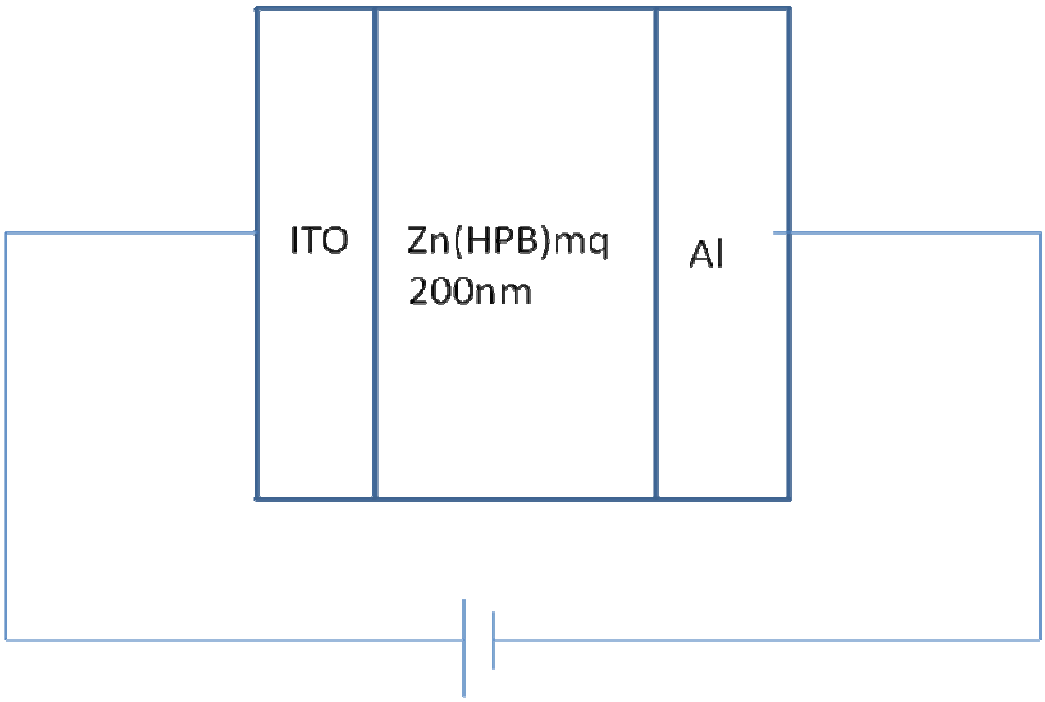

Figure 3.10: Electron only device for transport studies.

.

CHAPTER- 4

RESULT AND DISCUSSION

4.1 Thermal Characterization

Thermal characterization of the material has been done using thermo gravimetric analysis (TGA) technique and measure the change in weight of material as a function of temperature . In this technique a few milligram of substance in weight is heated at a constant rate of temperature under nitrogen atmosphere and note the change in weight at different temperature. Basically it gives the thermal stability of material. In the present work ,the thermo gravimetric analysis of CuPc and a Zinc complex namely Zn(HPB)mq before fabricating the device.

4.1.1 Thermo gravimetric analysis of Zn(HPB)mq

Thermo Gravimetric Analysis (TGA) of synthesized Zn(HPB)mq was carried out in temperature range 0-800^{o}C as shown in **figure 4.1**. The TGA plot shows a some weight loss around temperature 150 ^{0}C which due to some volatile impurities or moisture present in material but no weight loss in Zn(HPB)mq. At temperature around 350 ^{o}C the material degrade completely. Hence the material is stable upto 350^{o}C.

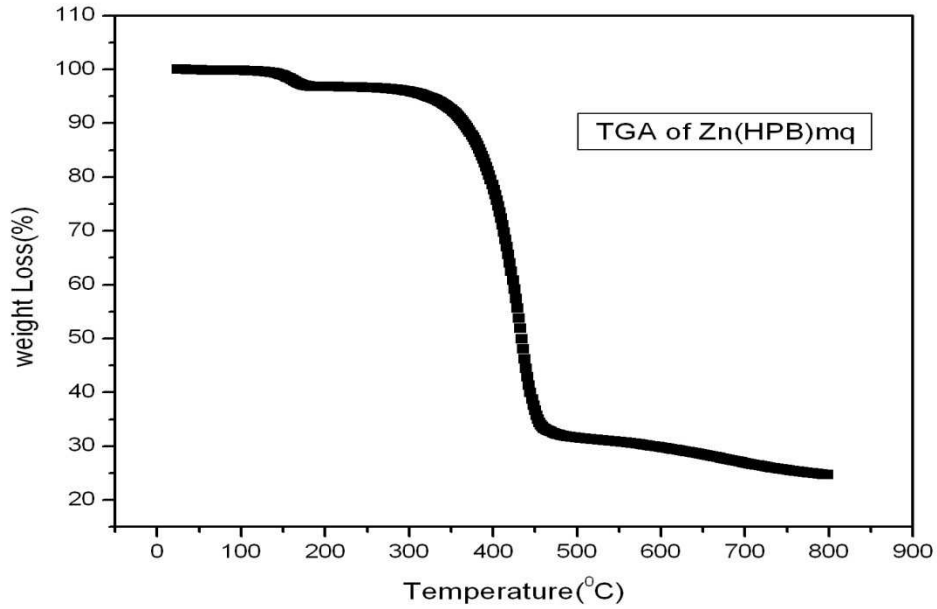

Figure 4.1: Thermo Gravimetric Analysis curve for Zn(HPB)mq

The high thermal stability of Zn(HPB)mq is an advantages in the fabrication of organic light emitting device.

4.1.2 Thermo gravimetric analysis of Copper Phthalocyanine

Thermo Gravimetric Analysis (TGA) of CuPc was carried out in temperature range 0-800^{o}C as shown in Figure 4.2. The TGA plot shows a complete weight loss at temperature around 450 ^{o}C . Hence the material is stable upto 450^{o}C.

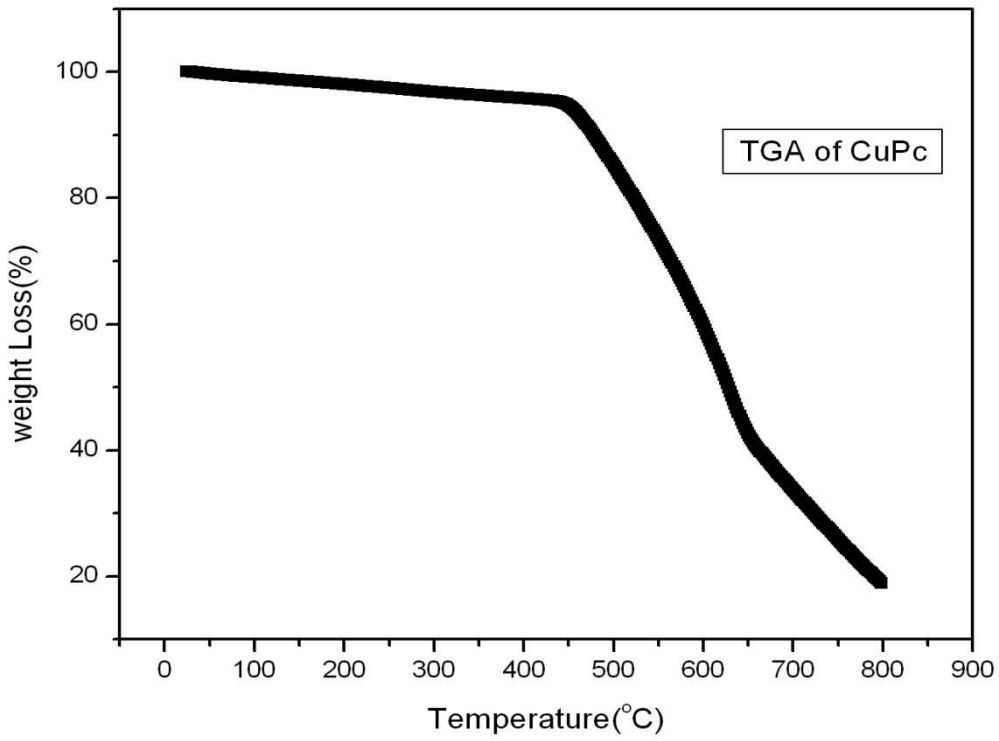

Figure 4.2: Thermo Gravimetric Analysis curve for Copper pthalocynine (CuPc)

4.2 Optical Characterization

UV-visible absorption spectra of the Zn(HPB)mq and CuPc were recorded on a Shimadzu UV-2401 spectrophotometer. The excitation and emission spectra of a solution of Zn(HPB)mq were recorded with a Fluorolog Spectrofluorometer (Horiba Jobin YVON Fluolog Model FL 3-11) at room temperature.

4.2.1 Optical Characterization of Zn(HPB)mq

The UV-Vis absorption and photoluminescence spectrum were measured in a solution of toulene Figure 4.3 and 4.4 shows the UV and PL spectra of Zn(HPB)mq respectively. The maxima of the UV-Vis absorption peaks of Zn(HPB)mq was observed at 380 nm, which is due to the π-π^* transition of aromatic ring. The peak of the PL

spectrum of Zn(HPB)mq was observed at 525 nm. This indicate the material emits the yellowish green colour.

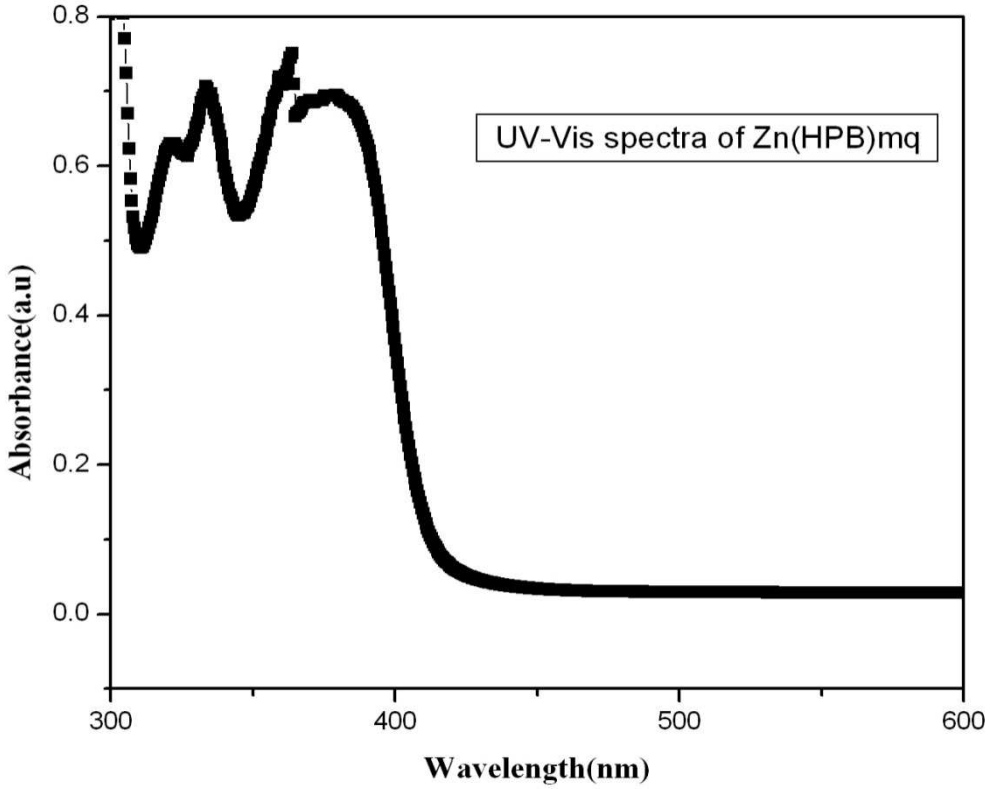

Figure 4.3: UV-Visible spectrum of Zn(HPB)mq.

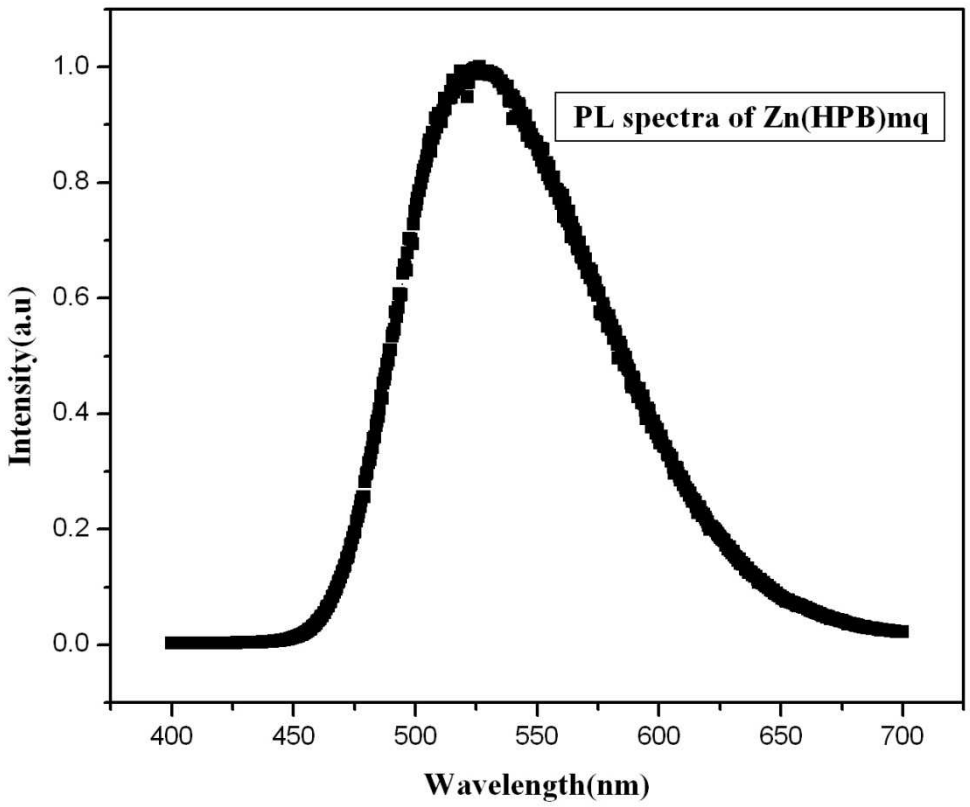

Figure 4.4: Photoluminescence spectrum of Zn(HPB)mq

4.2.2 Optical Characterization of Copper Pthalocynine (CuPc)

The UV-Vis absorption and photoluminescence spectrum were measured in a solution of ethanol Figure 4.5 & 4.6 shows the UV and PL spectra of CuPc respectively. The maxima of the UV-Vis absorption peaks of CuPc was observed at 270 nm. The peak of the PL spectrum of CuPc was observed at 410 nm.

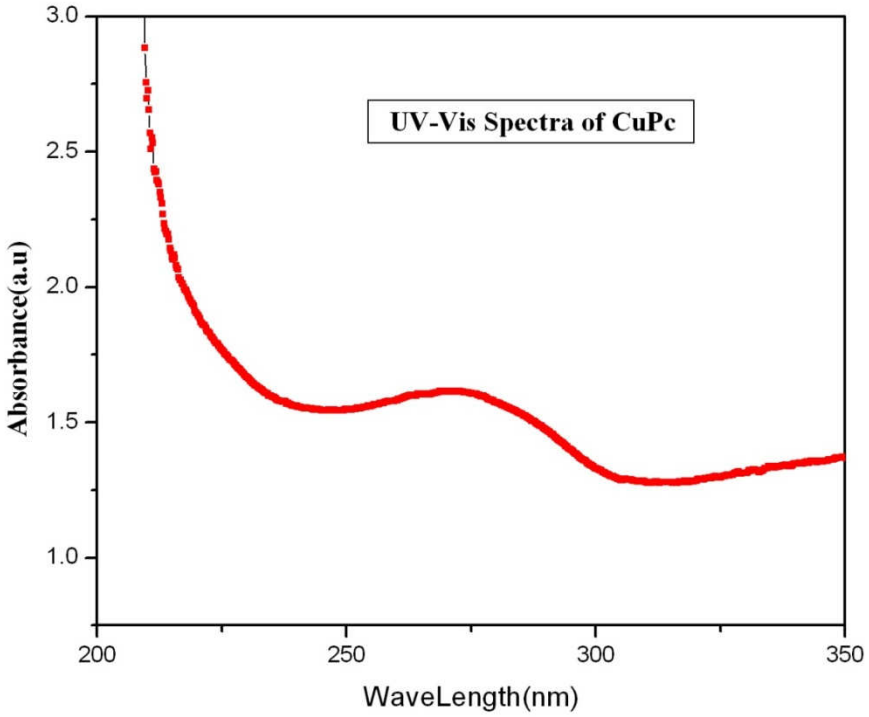

Figure 4.5: UV-Visible spectra of Copper pthalocynine (CuPc)

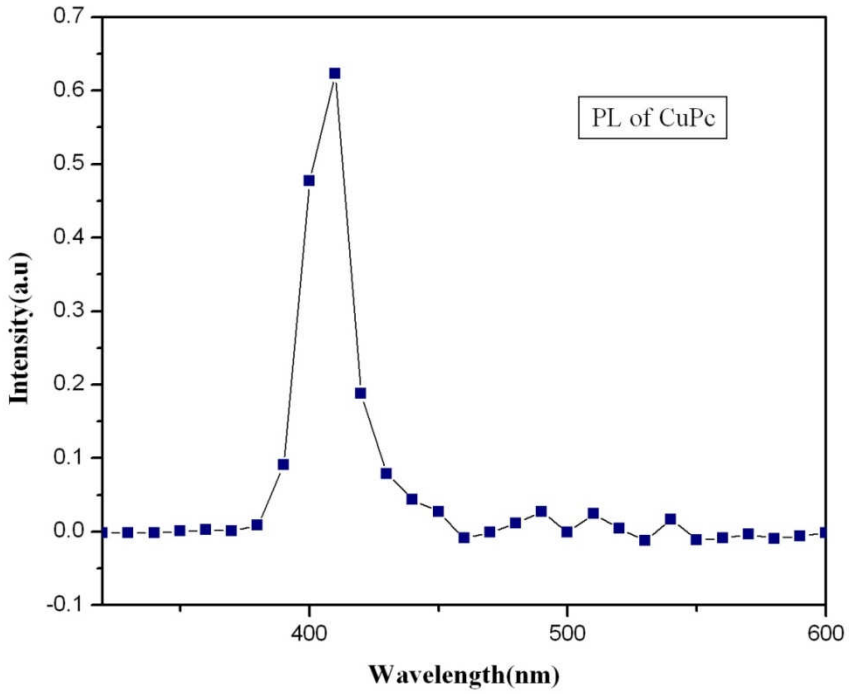

Figure 4.6: Photoluminescence spectra of Copper pthalocynine (CuPc)

4.3 Device Characterization:

The electroluminescent (EL) spectrum was recorded on a high-resolution spectrometer (Ocean Optics, HR-2000CG UV-NIR). The luminance–current–voltage (I-V-L) characteristics were measured using a luminance meter (LMT 1009) and a Keithley 2400 programmable voltage-current digital source meter.

4.3.1 Device characterization of Zn(HPB)mq

The EL spectra were recorded at various applied voltages **(Figure 4.7).**The EL intensity of the device increases with increase in voltage from 6V to 11 V, and the peak position remain unchanged at 545 nm.

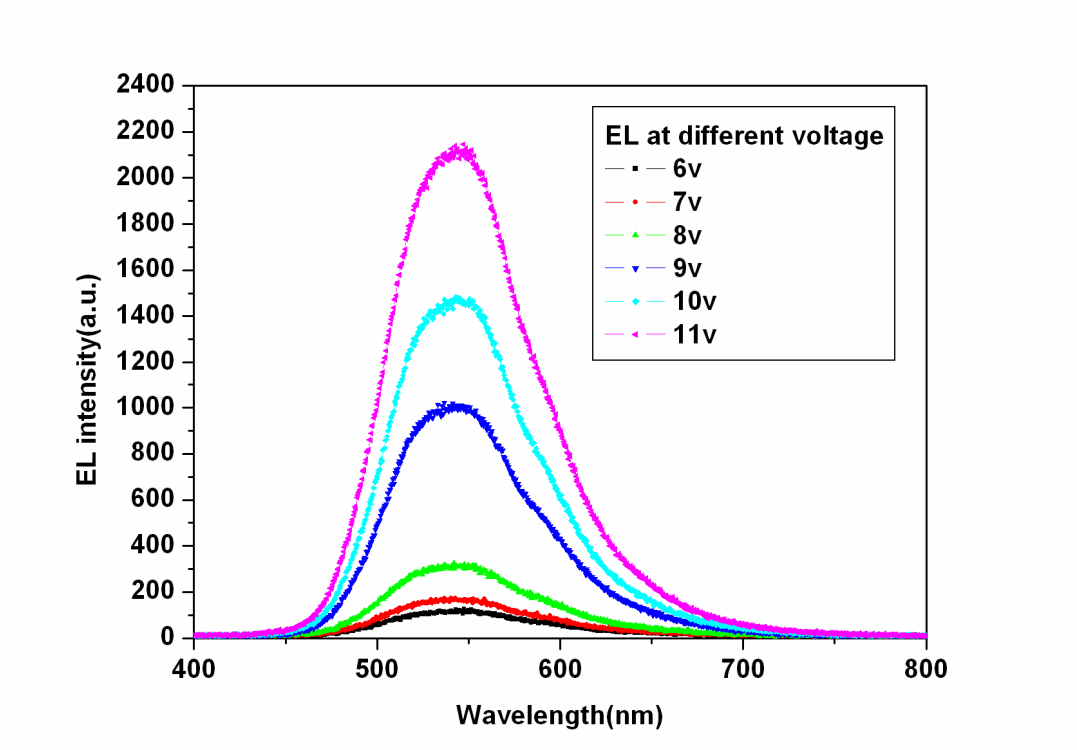

Figure 4.7: Electroluminescence – Wavelength curve at different voltages for Zn(HPB)mq

The current voltage (I-V) characteristic of the fabricated device was recorded by applying voltage across the device with ITO as an anode and Aluminium as cathode (forward bias) as shown in Figure 4.8. From Fig ure 4.8 the I-V characteristic it has been observed that the onset of light emission starts at about 4.5 V (threshold voltage). Above this voltage, the current increases non-linearly due to the space charge effects. Above the threshold voltage the device emits a yellowish green light. Below this voltage the I-V characteristics shows Ohmic current indicating the presence of thermally generated carrier. Figure 4.8 shows the current-voltage-luminescence curve for the device.

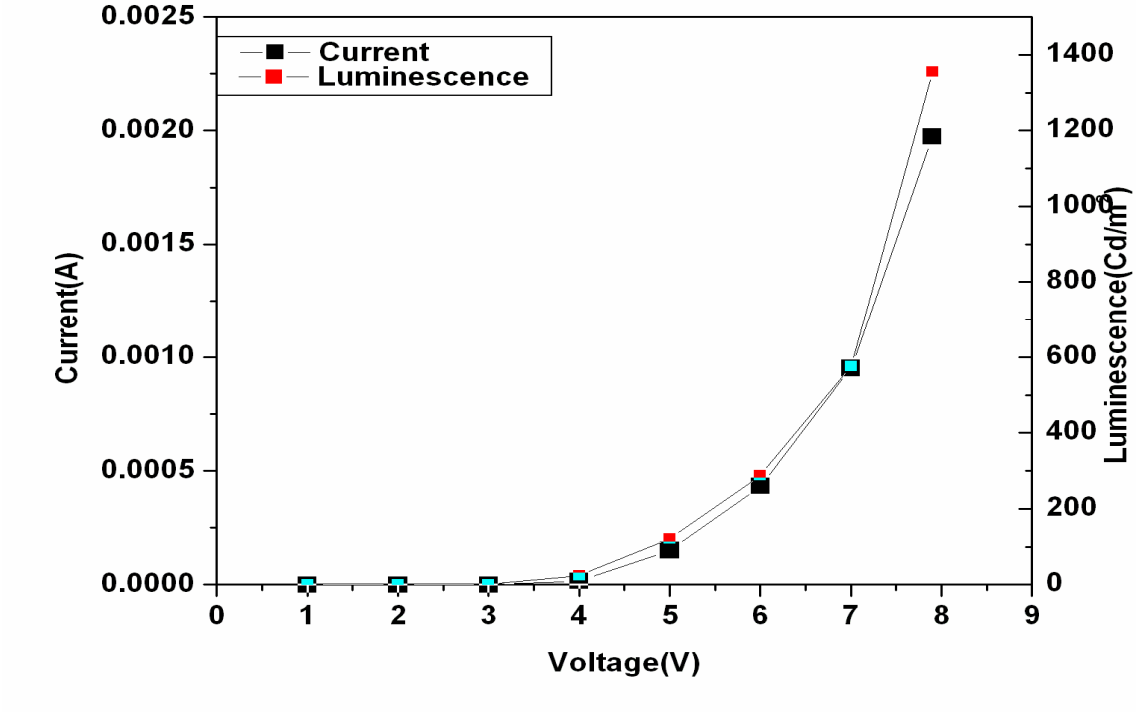

Figure 4.8: Current- Voltage- Luminescence curve for OLED device.

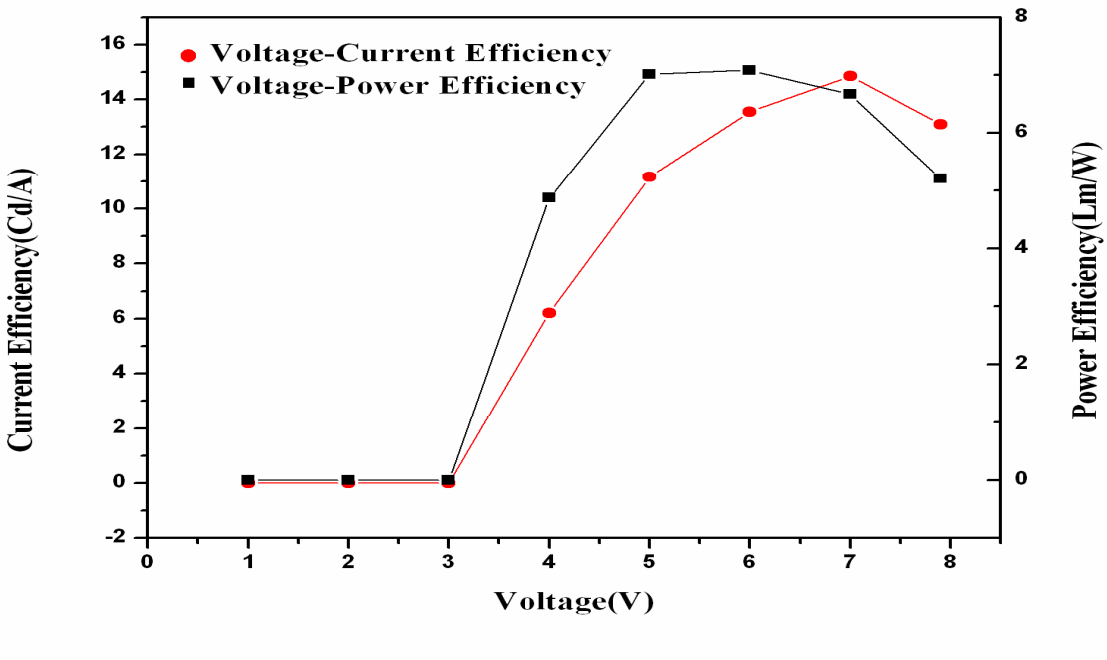

Figure 4.9: Current Efficiency- Voltage- Power Efficiency Curve of OLED Device

The maximum luminance in the EL cell was 1360 Cd/m^2 at 8 volts. The device shows maximum current efficiency 15 Cd/A and maximum power efficiency 7.1 lm/W at 6V as shown in Figure 4.9

4.4 Low Temperature transport studies of Organic material

In the following we will analyze our experimental results which were mainly obtained on single carrier device using analytic equations or simple numeric integration of the transport equations. A central question thereby will be whether the current in a device is injection limited or space charge limited and if the latter case applies, whether TCLC with an exponential trap distribution or a field and temperature dependent charge carrier nobilities play dominant role. It is shown that apart from the dependence of the current on voltage and temperature, the dependence on the thickness of the organic layer provides a unique criterion to distinguish between the underlying mechanisms. For clarity

we therefore briefly list the functional dependence of the current on the thickness at constant electric field for these three situations:

1) For purely injection limited behavior the current at constant field has no explicit thickness dependence(equation 4.1 &4. 2)

J =j(F)

$$j_{\mathrm{RS}} = A^* T^2 \exp\left(-\frac{\Phi_{\mathrm{B}} - \beta_{\mathrm{RS}}\sqrt{F}}{k_{\mathrm{B}} T} \right), \quad \text{----------4.1}$$

With the field F, Richardson constant $A^* = 4\pi m^* k_B^2 / h^3$(=120 A/($cm^2K^2$) for $m=m^*$) $ß_{RS}$ = sqrt($q^3/4\pi\varepsilon\varepsilon_o$) and zero field injection barrier Φ_B(q=elementary charge,m_0 free electron mass, k_B :Boltzmann constant, h:Plancks constant: relative permittivity,ε_0 are vacuum permittivity). The FN mechanism, on the other hand ignores Columbic effects and considers mere tunneling barrier into continuum states.

$$j_{\mathrm{FN}} = \frac{A^* q^2 F^2}{\Phi_{\mathrm{B}} \alpha^2 k_{\mathrm{B}}^2} \exp\left(-\frac{2\alpha \Phi_{\mathrm{B}}^{3/2}}{3qF} \right), \quad \text{----------4.2}$$

With $\alpha = \frac{4\pi\sqrt{2m^*}}{h}$.

2) For trap-free space-charge limited conduction with(or without) a field – dependent mobility the current at constant field scales with d^{-1} ,Where d is the thickness of device .

3) For trap-charge limited conduction with an exponential trap distribution and a field independent mobility the current at constant field scales with d^{-l} with $l > 1$.

4.4.1 Electron Only device

Electron only device with configuration ITO/Zn(HPB)mq(200nm)/Al has been fabricated and temperature dependent Current density-Voltage characteristics are shown in Figure 4.10.The electron are injected from Al electrode side.

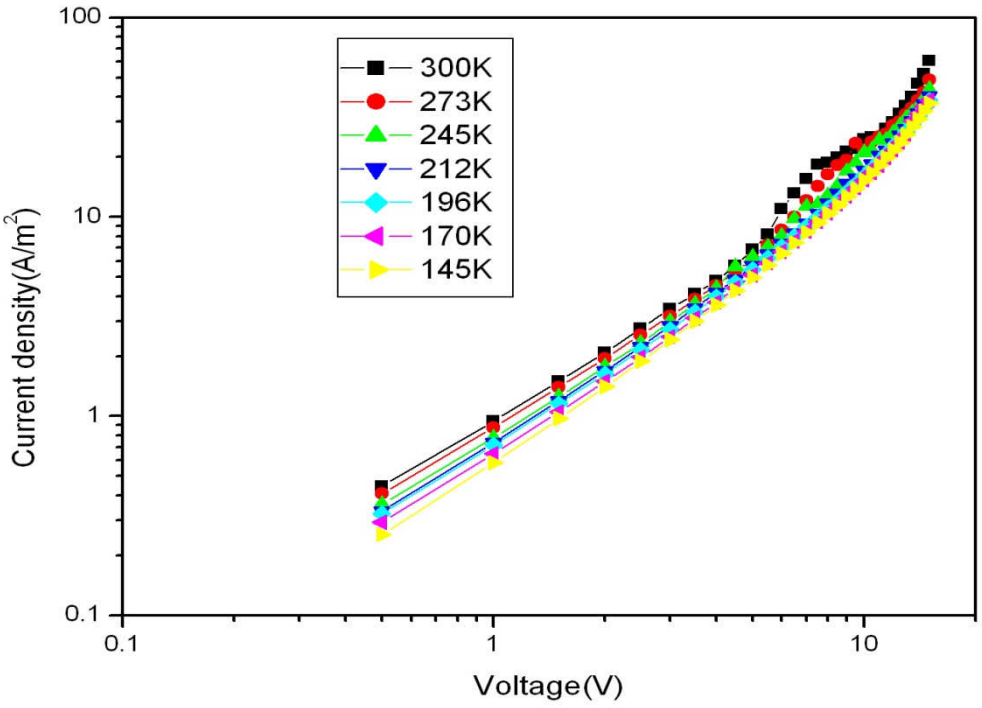

Figure 4.10: Current Density-Voltage (logJ-logV plot) characteristics of 200nm thick Zn(HPB)mq electron only device.

As the voltage is increased from 4V onwards, J is found proportional to the square of applied voltage, indicating the effect of space charge in the electrical transport process. The slope of 2 remained the same upto 15 Volts , suggesting field independent electron mobility in these samples**[81].** Hence at higher voltage space charge limited conduction takes place.

The current density–voltage expression in a space charge regime with charge trapping at discrete levels is given by the Mott–Gurney equation

$$J = \frac{9}{8}\varepsilon\varepsilon_0\theta\mu\frac{V^2}{d^3},$$

Where $\theta = n_0/(n_0 + n_t)$ or $\theta = p_0/(p_0 + p_t)$, where n_0 and p_0 are the free electron and hole densities and n_t and p_t are the trapped carrier densities, d, the thickness of the film, ε_0, the permittivity of free space, ε, the dielectric constant and μ, the charge carrier mobility. At constant temperature where θ remains constant and if μ remains field independent, the current density should scale inversely with the cube of thickness.

4.4.2 Hole only Device

Temperature dependent electrical properties of a hole only device with organic semiconductor Copper phthalocyanine (CuPc) has been studied extensively with the device configuration ITO/CuPc/Al. The work function of ITO and Al are 4.75 eV & 4.2 eV respectively. CuPc is a hole transport material with ionization potential and electron affinity of 4.8 eV and 3.1 eV respectively**[82].** The barrier height for hole is 0.05 ev as compared to electron 1.74eV. Figure 4.11 shows that current are strongly dependent on thickness .Hence the possibility of pure injection limited conduction is ignored. Figure 4.11 shows the current density at different thickness.

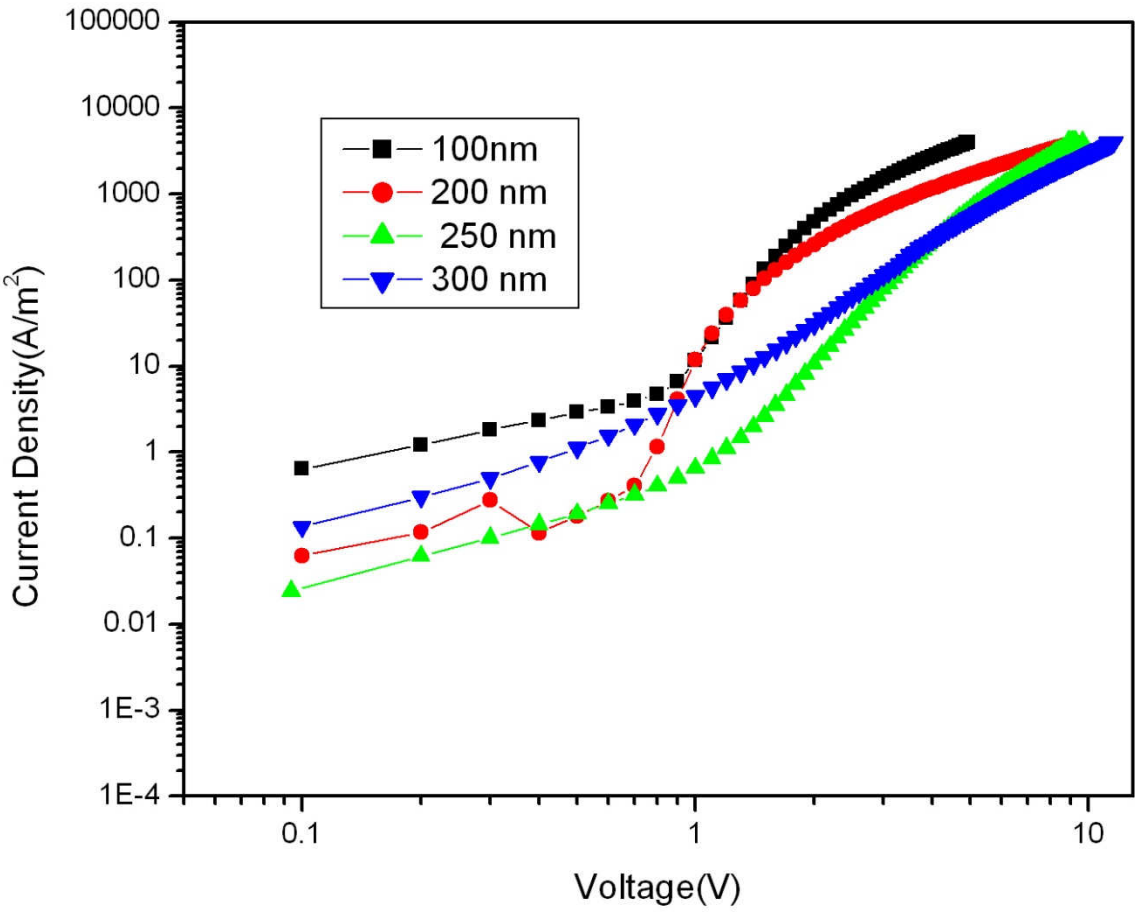

Figure 4.11: Current Density- Voltage curve for different thickness.

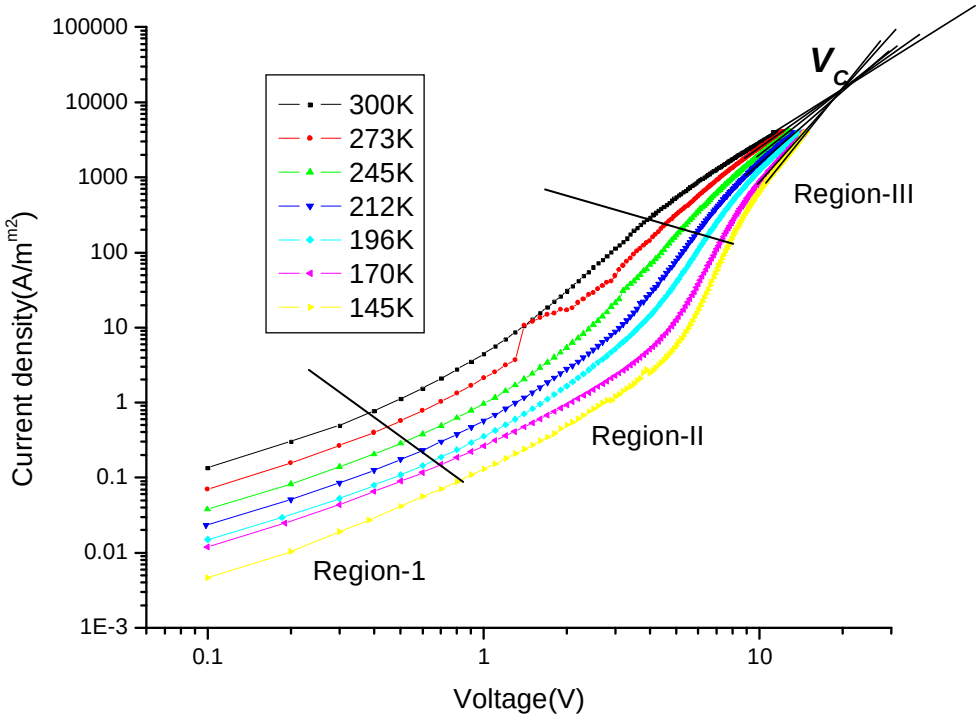

Figure 4.12: Current density -Voltage Characteristics(Log J –LogV plot) at different temperature for thickness 300 nm

For exponential distribution of traps the $I - V$ characteristics can be described by trap charge limited model where the $\log J - \log V$ curves can be divided into three distinct regions. (I) , (II), (III) as shown in Figure 4.12.

In region (I) the applied external electric field is small and the interface barrier blocks the charge injection; hence the number of charge carriers participating in the current does not increase. Current depends exclusively on applied field, and on the conductivity of the material. Conduction is due to the intrinsic thermally generated charge carriers, as well as due to some charges associated with the dopants, and obeys Ohm's law.

The region (II) is known as the trap filling region.When the applied voltage passes the threshold of blocking the number of charges, the total current increases with increase in voltage. It understand this as the filling of traps within the bulk where the bulk material accommodates this increase in charge carriers. Rapid increase in current with small increases in voltage is due to this increase in charge carrier density in the bulk. This region is characterized by $J = KV^{m}$, m is the slope. This is usually described by the power law which assumes the filling of traps distributed exponentially or uniformly within the band gap, the maximum density being at the band edge. The slope therefore can be used as a criterion for comparison of the stretching of the exponential distribution. Low slope implies gradual (extended) distribution, while higher slopes indicate sharp distribution.

Finally region (III) corresponds to trap free space charge limited current. Since the obtained slope in the double log plot is equal to 2 and is described by Child's law. Note that this law does not necessarily imply the absence of traps in the material, but rather that they are all filled.

At the bias voltage V_C all the traps are filled and E_F coincides with the valence band edge energy E_{vb} . V_C indicates the minimum voltage which is necessary to apply in order to fill up all existing traps at that temperature. Practically we expect the slope of the J(V) curve to transform to 2 as V_C is approached, in conformity with trap free SCLC. If the V_C is same for all temperature as shown in Figure 4.12, this indicates that the traps are so deep that at temperature considered, the energies k_BT are smaller than those required to fill up any significant number of traps.

Traps which are favorable energy states inside the band gap of the material can be shallow or deep or distributed in energy. Shallow or deep trap is defined depending on the position of the Fermi level with respect to the trap energy level. For hole traps if the Fermi energy level lies above the trap energy level it is called shallow trap, on the other hand if the Fermi energy level lies below the trap level, it is called deep trap with respect

to valance band (Figure 4.13). The reverse is true for electron with respect to conduction band edge**[83].**

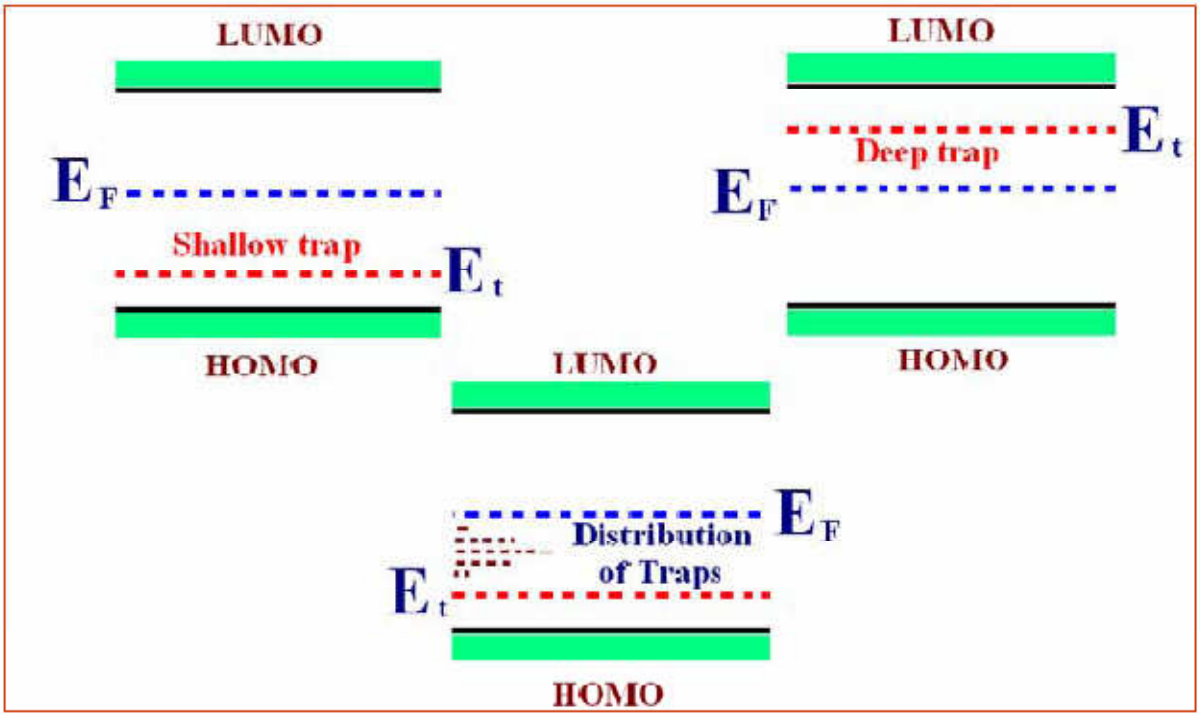

Figure 4.13: Schematic of typical hole traps.

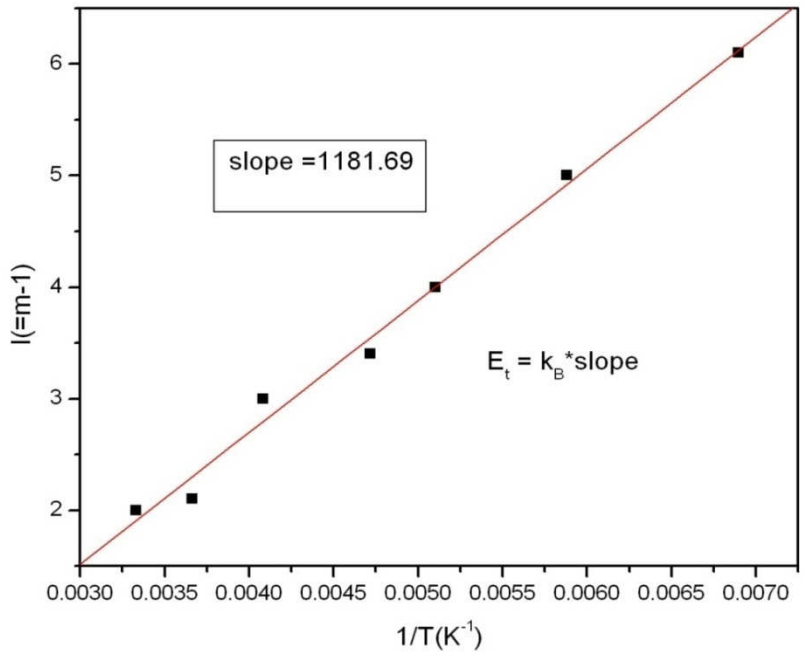

Figure 4.14: Slope Vs T^{-1} plot for ITO/CuPc/Al

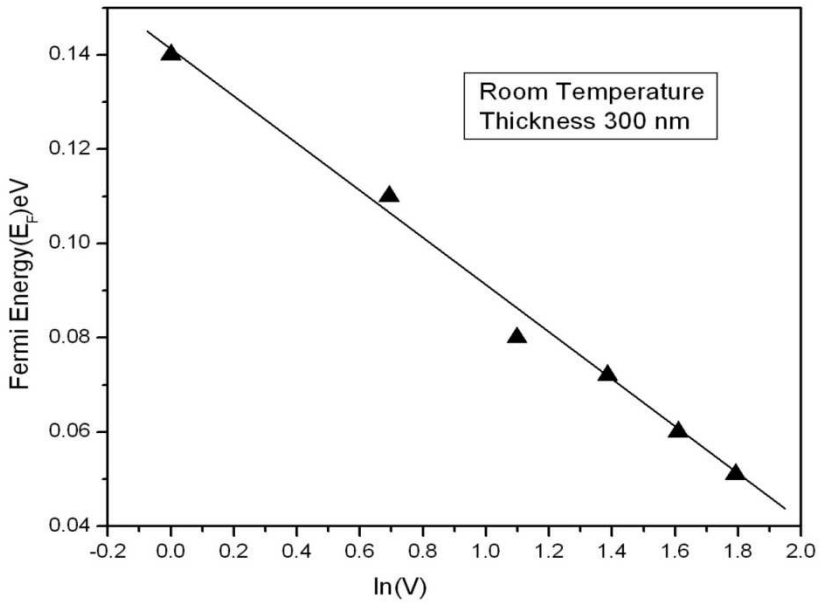

Figure 4.15: Fermi energy – Voltage (ln(V)) plot at room temperature(300K) for different voltage.

The trap energy(E_t) calculated using slope of curve (Figure 4.14) is 0.10 eV with the trap density 7.49 X $10^{16}cm^{-3}$ and the Fermi energy calculated (Figure 4.15) at lower voltage i.e. upto 2 volt is 0.14 which shows that the traps are shallow traps. The mobility at room temperature is 0.92 x 10^{-5} cm^3/V-s. At higher voltages the traps are deep with respect to valence band and the methods for calculating these parameters are given in *Chiguvare et.*al **[77].**

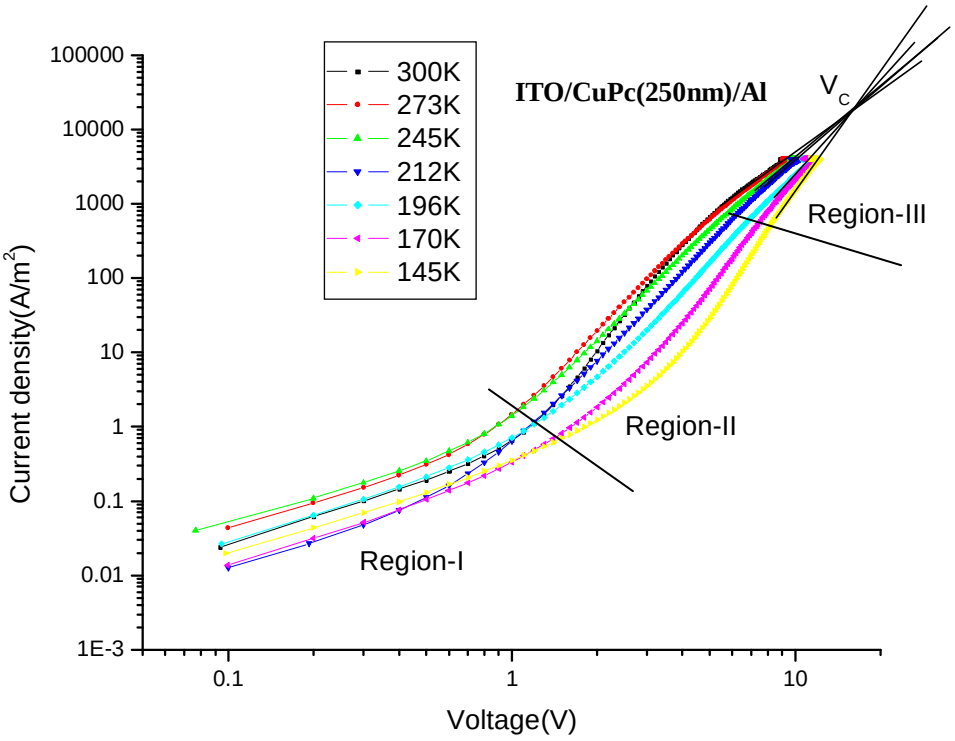

Figure 4.16: Current density-Voltage(logJ-LogV) characteristics at different temperature for thickness 250 nm.

For exponential distribution of traps the $I - V$ characteristics can be described by trap charge limited model where the Current Density − *V*oltage curves can be divided into three distinct regions. (I), (II), (III) as shown in Figure 4.16 .

In region (I) the applied external electric field is small and the interface barrier blocks charge injection; hence the number of charge carriers participating in the current does not increase. Conduction is due to the intrinsic thermally generated charge carriers, as well as due to some charges associated with the dopants, and obeys Ohm's law.

The region (II) is known as the charge injection limited and trap filling region. When the applied voltage passes the threshold of blocking the number of charges, the total current increases with increase in voltage. This region is characterized by $J = KV^{m}$, m is the slope. This is usually described by the power law which assumes the filling of traps distributed exponentially or uniformly within the band gap, the maximum density being at the band edge.

Finally region (III) corresponds to trap free space charge limited current. Since the obtained slope in the double log plot is equal to 2 and is described by Child's law. At the bias voltage V_C all the traps are filled and E_F coincides with the valence band edge energy E_{vb}. V_C indicates the minimum voltage which is necessary to apply in order to fill up all existing traps at that temperature. Practically we expect the slope of the J(V) curve to transform to 2 as V_C is approached, in conformity with trap free SCLC. As shown in figure the V_C is same for all temperature and the crossover voltage is16.11 volts as shown in Figure 4.16. The hole mobility is $0.52X10^{-5}$ cm^{-3}/V-s at room temperature with trap density 4.81×10^{5} cm^{-3}.

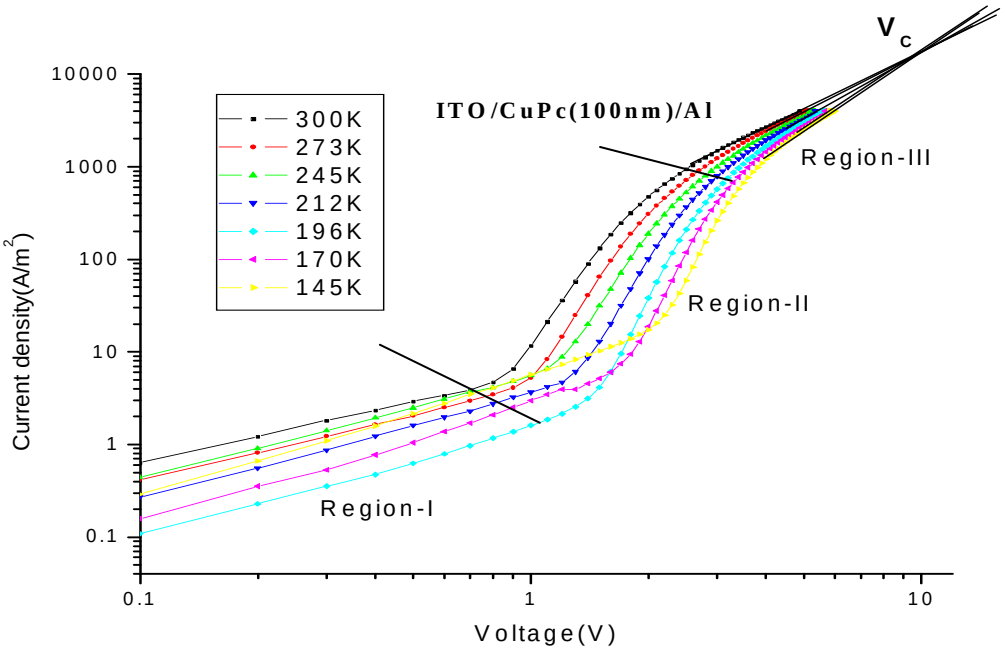

Figure 4.17: Current density-Voltage characteristics at different temperature for thickness 100 nm.

In above figure region-1 shows that the current is linearly change with voltage and hence obey ohm's law . As we increase the voltage region –II is reached, here the conduction mechanism is bulk trap charge limited conduction and obey $J=KV^m$ where m (m>2) is slope of the curve .

Region-III shows the trap free space charge limited conduction and follow power square law i.e. $J = K V^m$, m=2. V_c shows crossover voltage at which current density becomes independent of temperature. The hole mobility is 0.09 X 10^{-5} cm^{-3}/V-s at room temperature with trap density 1.78X 10^{17} cm^{-3}.

CHAPTER-5

SUMMARY AND FUTURE SCOPE

5.1 Summary

One of the most exciting opportunities in optoelectronics currently is device based on organic materials. These have many advantages, primarily: lower-technology processing with less sensitivity to processing environment, flexibility and the opportunity to apply the enormous power of organic synthesis to tailoring the properties of the materials to specific applications. Furthermore, organics can emit light directly as do conventional cathode-ray-tube and plasma display panels, rather than relying on back-lighting systems such as are used in liquid-crystal displays. One can imagine these technologies leading to poster size televisions which can be rolled up and stored in mailing tubes, or unrolled and thumb-tacked to a wall. The materials are already being applied in compact light weight, power efficient light emitting device in small areas such as cell-phone displays. The primary problem with all organic devices is stability. When carriers are injected in these materials, sometimes a molecule falls apart.

An organic electroluminescent material, zinc complex {2-(2-hydroxyphenyl) benzoxazole) 2-methyl -8-hydoxyquinoline}Zinc [Zn(HPB)mq] was synthesized and characterized using different spectroscopic techniques. The excitation and emission spectra of the complex were studied. The light emitting diode with configuration ITO/α-NPD/Zn(HPB)mq/LiF/Al have been fabricated and the complex was employed as an emitting layer in fabricating OLEDs that had emission peak at 545 nm with a bright yellowish green color. electroluminescence and photoluminescence characteristics were approximately matching. It has been found that the complex is a good electroluminescent material to be used for device applications.

The temperature dependent transport properties of this zinc complex with configuration ITO/Zn(HPB)mq(200 nm)/Al has been studied. Both type of charge carrier are injected in this material from both the electrode but due to high injection barrier for hole, it shows better electron transport. Hence it has been considered as a electron only device and study the Low temperature I-V characteristics which shows ohmic contact at lower voltage and trap filling space charge limited conduction at higher voltages.

The low temperature I-V characteristics of hole only device using organic material Copper Phthalocyanine (CuPc) with different thickness have been studied and observed the effect of thickness on the current density. The device configuration is ITO/CuPc/Al. Copper Phthalocyanine (CuPc) shows a better hole transport properties as compared to electron. For all thickness ohmic conduction has been observed at lower voltage and at slightly higher voltages trap charge limited conduction(TCLC) mechanism with slope >2 has been observed .At much higher voltage we observed trap free space charge limited conduction(TFSCLC) having slope 2, further increase in voltage , a point is reached at which all the curve meet, this point is called crossover voltage or critical voltage (V_c) and At this point current becomes independent of temperature.

5.2 Future scope

This research opens up some new avenues for future research in the design and development of new optoelectronic devices based on small molecules and other Conjugated Polymers. The studies presented in thesis further suggest that there are areas of academic and technological interest. Some of the areas are mentioned as follows

1) In the present work, Zinc complex (Zn(HPB)mq) has been used as emissive layer in fabricating the OLED device and shows good electroluminescence properties. The effect of attachment of methyl groups and different ligand to the some other metal complexes (Al, Cd,Be,B,Pt) and other rare earth elements) could be tried for optimizing quantum efficiency, brightness and operating voltages.

2) Temperature dependent photoluminescence could also be carried out in order to get information about the variation of the traps ,excitonic vibrations etc.

3) Temperature dependent transport studies could be performed deeply for getting the information about the conduction mechanism i.e. Injection limited conduction and bulk limited conduction , since it pave the way for better device fabrication.

4) Another possible area of future research work will be to reduce the interface defects which form during OLED fabrication in order to increase current densities which will eventually improves the device efficiency.

REFERENCES

[1] M. Pope, H. Kallmann, and P. Magnante, J. Chem. Phys. **38**, 2042 (1963).

[2] W. Helfrich and W.G. Schneider, Phys. Rev. Lett. **140**, 229 (1965).

[3] E.A. Silinsh. Organic Molecular Crystals. Springer, Berlin 1980.

[4] M. Pope and C.E. Swenberg. Electronic Processes in Organic Crystals. Clarendon Press, Oxford 1982.

[5] D.F.Williams and M. Schadt, Proc. IEEE (Lett.) **58**, 476 (1970).

[6] C. K. Chiang, C. R. Fincher, Jr., Y. W. Park, A. J. Heeger, H. Shirakawa, E. J. Louis, S. C. Gau, and Alan G. MacDiarmid, Phys. Rev. Lett. **39**, 1098 (1977).

[7] T.A. Skotheim (Ed.). Handbook of Conducting Polymers. M. Dekker, New York 1986.

[8] C.W. Tang, Appl. Phys. Lett. **48**, 183 (1986).

[9] H. Koezuka, A. Tsumara, and T. Ando, Synth. Met. **18**, 699 (1987).

[10] J.H.Burroughes, C.A. Jones, and R.H. Friend, Nature **335**, 137 (1988).

[11] G. Horowitz, D. Fichou, X.Z. Peng, Z. Xu, and F. Garnier, Solid State Communications **72**, 381 (1989).

[12] C.W. Tang and S.A. VanSlyke, Appl. Phys. Lett. **51**, 913 (1987).

[13] C.W. Tang and S.A. VanSlyke, J. Appl. Phys. **65**, 3610 (1989).

[14] J.H. Burroughes, D.D.C. Bradley, A.R. Brown, R.N. Marks, K. Mackay, R.H. Friend, P.L. Burn, and A.B. Holmes, Nature **347**, 539 (1990).

[15] D. Braun and A.J. Heeger, Appl. Phys. Lett. **58**, 1982 (1991).

[16] Pioneer Co. (Japan). In November 1997 Pioneer Co. in Japan commercialized a monochrome 256x64 dot matrix OLED display for automotive applications.

[17] Materials Today, September 2004: C. Reese et al. p. 20-27; I.D.W. Samuel et al. p. 28–35; N.S. Sariciftci p. 36-40; J.K. Borchardt p. 42–46 (www.materialstoday.com)

[18] M. Pope and C.E. Swenberg. Electronic Processes in Organic Crystals and Polymers. Oxford University Press, Oxford 1999.

[19] R. Farchioni, G. Grosso (Eds.), Organic Electronic Materials, Springer 2001.

[20] F. Faupel, C. Dimitrakopoulos, A. Kahn, Org. Elect., Special Issue of J.Mater.Res.**19,** 7,(2004).

[21] R. H. Friend , Nature (London) **397**, 121 (1999).

[22] M. A. Baldo, Nature (London) **395**, 151 (1998).

[23] D.G.Lidzey, D.D.C. Bradley, S.F. Alvarado, and P. F. Seidler; Nature (London) **386**, 135 (1997).

[24] J.J.M. Halls, C.A. Walsh, N.C. Greenham, E.A. Marseglia, R.H. Friend, S.C. Moratti & A.B. Holmes, Nature **376**, 498 (1995).

[25] G. Yu, J. Gao, J. C. Hummelen, F. Wudl, and A. J. Heeger, Science **270**, 1789(1995).

[26] J. J. M. Halls , Nature (London) **376**, 498 (1995).

[27] C. D. Dimitrakopoulos and D.J. Mascaro, IBM, J. Res. & Dev. **45**, (2001).

[28] B. Crone , Nature (London) **403**, 521 (2000).

[29] C. D. Dimitrakopoulos, S. Purushothaman, J. Kymissis, A. Callegari, and J. M. Shaw, Science **283**, 822 (1999).

[30] Joseph Shinar, "Organic Light Emitting Devices , A survey", Springer-Verlag New York, Inc. (2004).

[31] R. Friend, J. Burroughes and T. Shimoda, Physics World, **35**-40 (1999).

[32] Organic Light emitting diodes (OLEDs) for General Illumination Update 2002 Published by optoelectronics Industry Development Association (www.oida.org)

[33] S.M.Sze ,Physics of Semiconductor Devices, Wiley ,New York,1981

[34] N.F Mott ,R.W.Gurney, Electronic Processes in Ionic Crystal,Clarendon Press Oxford 1940

[35] Thesis entitled Carrier Injection& Transport in small molecule Organic Light emitting diode by\ Haichaun Mu, Department of Electrical and Computer Engineering , University of Cincinnati

[36] P.M. Murgatroyd , J.Phys.D: Appl. Phys**. 3,** 151(191)

[37] W. R. Salaneck and J. L. Brédas, Adv. Mater. **8**, 48 (1996).

[38] J. Blochwitz, T. Fritz, M. Pfeiffer, K. Leo, D. M. Alloway, P. A. Lee, and N. R. Armstrong, Org. Elect. **2**, 97(2001).

[39] X. Crispin, V. Geskin, A. Crispin, J. Cornil, R. Lazzaroni, W. R. Salaneck, and J.L. Brédas, J. Am. Chem. Soc. **124**, 8131(2002).

[40] H. Ishii, J. Lumines **87**, 61 (2000).

[41] H. Ishii, K. Sugiyama, E. Ito, and K. Seki, Adv. Mater. **11**, 605 (1999).

[42] S. Kera, Y. Yabuuchi, H. Yamane, H. Setoyama, K. K. Okudaira, A. Kahn, and N. Ueno, Phys. Rev. B **70**, 085304 (2004).

[43] H. Peisert, M. Knupfer, F. Zhang, A. Petr, L. Dunsch, and J. Fink, Surf. Sci. 566-568, **554** (2004).

[44] W. Osikowicz, X. Crispin, C. Tengstedt, L. Lindell, T. Kugler, and W. R. Salaneck, Appl. Phys. Lett. **85**, 1616 (2004).

[45] A. J. Mäkinen, I. G. Hill, R. Shashidhar, N. Nikolov, and Z. H. Kafafi, Appl. Phys. Lett. **79**, 557 (2001).

[46] L. Chkoda, Synth. Met. **111**, 315 (2000).

[47] C. Giebeler, H. Antoniadis, D. D. C. Bradley, and Y. Shirota, J. Appl. Phys. **85**, 608 (1999).

[48] C. Ganzorig, K.-J. Kwak, K. Yagi, and M. Fujihiraa, Appl. Phys. Lett. **79**, 272 (2001).

[49] S. Besbes, A. Ltaief, K. Reybier, L. Ponsonnet, N. Jaffrezic, J. Davenas, and H. Ben Ouada, Synth. Met. **138**, 197 (2003).

[50] R. A. Hatton, S. R. Day, M. A. Chesters, and M. R. Willis, Thin Solid Films **394**, 292 (2001).

[51] P. K. H. Ho, M. Granstroem, R. H. Friend, and N. C. Greenham, Adv. Mat. **10**, 769 (1998).

[52] X. H. Sun, L. F. Cheng, M. W. Liu, L. S. Liao, N. B. Wong, C. S. Lee, and S. T. Lee, Chem. Phys. Lett. **370**, 425 (2003).

[53] K. Sugiyama, H. Ishii, Y. Ouchi, and K. Seki, J. Appl. Phys. **87**, 295 (2000).

[54] C. C. Wu, C. I. Wu, J. C. Sturm, and A. Kahn, Appl. Phys. Lett. **70**, 1348 (1997).

[55] [Abd R. B. M. Yusoff, W. J. da Silva, J. P. M. Serbena, M. S. Meruvia, and I. A. Hümmelgen Appl. Phys. Lett. **94**, 253305 (2009).

[56] Wolfgang Brutting, Stefan Berlab , Org. Elect. **2**, 1 (2001).

[57] Christoph Brabee, Vladimir Dyakonov, Organic Photovoltaic's, Springer Verlag(2003)

[58] C. D. Dimitrakopoulos, IBM J. Res. & Dev. Vol. 45 No. 1 , 2001

[59] M. Pope, H. P. Kallmann, P. Magnante, J. Chem. Phys., **38**, 2042 (1963).

[60] J. H. Burroughes, D. D. C. Bradley, A. R. Brown, R. N. Marks, K. Mackay, R. H.Friend, P. L. Burns, A. B. Holmes, Nature, **347**, 539(1990).

[61] Heqing Tang,Ke Xu,Lihua Zhu, J. Lumines.**118,** 39 (2006).

[62] J J Andre, J Simon, R Even, B. Boudjema, G. Guillaud and M. Maitrot, Synth. Met. **18,** 683(1987).

[63] N. El-Khatib, B. Boudjema, G. Guillaud and M. Maitrot ,*J*. Less-Common Met. **143** 101(1988).

[64] M.A. Khan, W. Xu, K. Haq, Y. Bai, X. Y. Jiang, Z. L. Zhang, and, W. Q. Zhu, Semicond. Sci. Technol. **23**, 055014(2008).

[65] S. A. VanSlyke, C. H. Chen and C. W. Tang Appl. Phys. Lett. **69,** 2160(1996)

[66] Y. Shirota, Y. Kuwabara, H. Inada, T. Wakimoto, H. Nakada,Y. Yonemoto, S. Kawami and K. Imai , Appl. Phys. Lett .**65 ,** 807(1994)

[67] Z. B. Deng, X. M. Ding, S. T. Lee and W. A. Gambling Appl.Phys. Lett. **74,** 2227(1999)

[68] E.Z. Faraggi, H. Chayet, G. Cohen, R. Newman, Y. Avny, D. Davidov, Adv Mater.**7**,742 (1995).

[69] J. H. Burroughes, D. D. C. Bradley, A. R. Brown, R. N. Marks, K. Mackay, R. H. Friend, P. L. Burns, A. B. Holmes, Nature, **347**, 539(1990).

[70] E.Z. Faraggi, H. Chayet, G. Cohen, R. Newman, Y. Avny, D. Davidov, Adv Mater.**7**, 742 (1995).

[71] M. Berggren, O. Inganas, G. Gustafsson, M.R. Anderson, T. Hjertberg. O. Wennerstrom, Nature, **372**, 444 (1994).

[72] W. Paul, M. Blom, Marc J.M., de jong and Coen T.H.F. Liedenbaum, Polym. Adv. Technol., **9**, 390 (1998).

[73] N. K. Patel, S. Cinà, and J. H. Burroughes, IEEE J. Selected topics Quant. Elec. **8,** 346 (2002)

[74] I. D. Parker, J. Appl. Phys. **75**, 1656 (1994).

[75] P. W. M. Blom, M. J. M. de Jong, and S. Breedijk, Appl. Phys. Lett.,**71**, 930 (1997).

[76] P. S. Davids, Sh. M. Kogan, I. D. Parker, and D. L. Smith, Appl. Phys. Lett., **69**, 2270 (1996).

[77] Z. Chiguvare and V. Dyakonov , Physical Review B, **70**, 235207 (2004).

[78] www.physicscourses.okstate.edu

[79] Mark Fox, "Optical absorption of solids", Oxford University Press Inc., (2001).

[80] http://www.impactanalytical.com/tga.html

[81] V. K. Rai,R. Srivastava, G. Chauhan, M.N. Kamalasanan , J.Phys.D:Appl.Phys.**41**,195109(2008)

[82] S.R.Forest,G.Parthasarathy,P.E.Burrows, Appl. Phys.Lett. **72**,2138(1998).

[83] M.A.Lampert and P.Mark,"Current Injection in Solids"Academic press New York(1970)